Proc. Lunar Planet. Sci., 12B (1981), p. 67–97.
Printed in the United States of America.

A comparative Rb–Sr, Sm–Nd, and K–Ar study of shocked norite 78236: Evidence of slow cooling in the lunar crust?

L. E. Nyquist,[1] W. U. Reimold,*[2] D. D. Bogard,[1] J. L. Wooden,[3] B. M. Bansal,[3] H. Wiesmann,[3] and C.-Y. Shih[3]

[1]NASA Johnson Space Center, Houston, Texas 77058 [2]Universität Münster, 4400 Münster, F. R. Germany [3]Lockheed, 1830 NASA Road 1, Houston, Texas 77058

Abstract—Rb–Sr, Sm–Nd, and ^{39}Ar–^{40}Ar isotopic data are reported for mineral separates of shocked cumulate norite 78236. Petrographic observations are reported to document the mineralogy and degree of shock metamorphism of the samples analyzed. All minerals have been shocked to a moderate degree (~30 GPa) with local areas of more intense shock (up to ~50 GPa). Veins of solidified melt most probably have been developed *in situ*. The shock features could have been produced either in a single event or in two events; our observations favor a single event. All three isotopic systems are disturbed to some extent. The most severe disturbances were observed for melt glass and some pyroxene separates analyzed for Rb–Sr and for the first small amounts of Ar released in temperature steps below 950°C from a maskelynite separate. An upper limit to the time of occurrence of the most recent thermal event of 3.5 AE can be inferred from the Rb–Sr and ^{39}Ar–^{40}Ar data. This event is identified with thermal annealing following the (most recent?) shock event. Concordant Rb–Sr and Sm–Nd ages calculated from pyroxene-whole rock tie lines and the average ^{39}Ar–^{40}Ar age of the last ~84% of the ^{39}Ar release from maskelynite support a crystallization age of ~4.4 AE for 78236. The Rb–Sr and Sm–Nd ages determined by the most retentive samples are 4.38 ± 0.02 AE ($\lambda(^{87}Rb) = 0.0139\ AE^{-1}$), and 4.43 ± 0.05 AE ($\lambda(^{147}Sm) = 0.00654\ AE^{-1}$), respectively. Apparent ^{39}Ar–^{40}Ar ages of 4.19–4.56 AE are obtained between 16% and 92% of the ^{39}Ar release, and the average ^{39}Ar–^{40}Ar age of the last 84% of the ^{39}Ar release is 4.39 AE (K–Ar constants from Steiger and Jaeger, 1977). Slightly younger ages are obtained for less severe data selection criteria. Thus, linear regressions including data which are probably partially reset yield apparent ages of 4.27 ± 0.11 AE and 4.33 ± 0.09 AE for the Rb–Sr and Sm–Nd data, respectively. The total K–Ar age of the maskelynite separate is 4.26 AE, which establishes a lower limit to the crystallization age. We believe that these latter ages are biased toward values younger than the true crystallization age; however, a crystallization age ≥ 4.26 AE is clearly confirmed. We find initial isotopic ratios I(Sr, 4.38) = 0.69907 ∓ 2 and I(Nd, 4.43) = 0.50609 ∓ 7. The deviation of I(Nd) from chondritic evolution is ϵ(Nd, 4.43) = 0.8 ± 0.4 parts in 10^4.

We suggest that some of the observed isotopic disturbances were caused by slow cooling of 78236 subsequent to its formation deep within the lunar crust and examine the consequences of this hypothesis using currently available diffusion data. These considerations suggest that isotopic systems can be kept open for long periods (~0.5 AE) for samples of deep crustal origin. Whether 78236 actually underwent such a slow cooling is unclear at this time.

INTRODUCTION

Three samples (78235, 78236, 78238) were chipped from the top of a $30 \times 55 \times 55\ cm^3$ norite boulder at Station 8 by the Apollo 17 Landing Team. From the geological setting of the boulder, astronauts Schmitt and Cernan concluded that this shattered and largely glass-coated boulder had arrived at its present site via impact-generated ballistic transport. Therefore, this norite, which is unique among all returned lunar samples, cannot be correlated to the geology of the Apollo 17 landing area. From textural evidence Jackson *et al.* (1975) concluded that this coarse-grained, cumulus-textured rock formed at a depth of 8–30 km in the lunar crust and suggested that it was excavated by a large basin-forming impact event.

*Also at Lunar and Planetary Institute, 3303 NASA Road One, Houston, Texas, 77058.

Sample 78236, the object of this study, was taken from the south edge of the boulder's top side and consists of a $7.5 \times 2.0 \times 5.5\ cm^3$ rock covered with glass on all but one side. Three subsamples of 78236 were provided to the Lunar Norite Consortium for isotopic, chemical, and petrographic investigation: 78236,3; 78236,4; and 78236,8. Thin sections ,8A1; ,8B1; and ,8B2 were prepared for petrographic studies.

Samples of 78235 and 78238 have been extensively studied before by various authors: Jackson *et al.* (1975)—structure, petrography; McCallum *et al.* (1975)—petrography; Winzer *et al.* (1975)—major and trace element chemistry; Sclar and Bauer (1975, 1976)—shock history; El Goresy *et al.* (1976)—petrography; Mehta and Goldstein (1980)—metal petrogenesis. However, the only previous isotopic analysis of this norite is the Sm–Nd study by Carlson and Lugmair (1981) of 78236. These authors found evidence of disturbance in the Sm–Nd systematics and interpreted their data as indicating a crystallization age of about 4.34 AE. The crystallization age has important consequences for hypotheses of lunar evolution and for the petrogenesis of this rock type. Thus, additional isotopic studies seemed justified.

We report here a comparative Rb–Sr, Sm–Nd, and ^{39}Ar–^{40}Ar study of norite 78236. An important aspect of our study was that Rb–Sr and Sm–Nd analyses were performed on the same sample solutions. In a study of the shergottite meteorites, we have shown that the Rb–Sr system is considerably more susceptible to disturbance associated with shock metamorphism than is the Sm–Nd system (Nyquist *et al.*, 1979b; Shih *et al.*, 1981; see also Lugmair and Scheinin, 1975, and Unruh *et al.*, 1977 for comparative isotopic studies on the Stannern and Pasamonte meteorites, respectively). Therefore, samples showing little or no disturbance of the Rb-Sr system may reasonably be expected to show no disturbance of the Sm-Nd system. Thus, on the one hand, the Rb-Sr data may be used as a filter on the Sm-Nd data to obtain the best possible estimate of the crystallization age of 78236. On the other hand, the Rb-Sr system might have been completely reset to the time of shock metamorphism as found for the shergottites. This turned out not to be the case, and most Rb-Sr data are only slightly more disturbed than the corresponding Sm–Nd data.

Because of the low diffusion rates expected for Sr and Nd in pyroxene (Hart, 1964; Hofmann and Magaritz, 1975, 1977) and the large pyroxene grain size, it is difficult to ascribe all of the isotopic disturbances to post-shock thermal metamorphism. This is also true for variations in the ^{39}Ar–^{40}Ar age spectrum above 1100°C. We thus suggest that some of the isotopic disturbances result from slow cooling at considerable depth in the lunar crust. Because the observed isotopic disturbances are very small, it is not possible to resolve the extent of re-equilibration derived from slow-cooling from that due to excavation-induced disturbances. Calculations are presented which show the influence of diffusion rate and grain size on closure temperature at a depth of 50 km in the moon.

PETROGRAPHIC DESCRIPTION AND SAMPLE PREPARATION

Petrography

The Station 8 norite boulder displays a pronounced cumulative texture (McCallum *et al.*, 1975; Jackson *et al.*, 1975). Generally, this rock is very coarse-grained (up to 5 mm grain size), but post-cumulate grains as small as 0.3 mm have been described as well. A subophitic texture is formed by nearly equal amounts of subhedral to euhedral plagioclase and orthopyroxene. A petrographic comparison of our samples of 78236 with the previously described chips 78235 and 78238 shows that all three specimens display a generally consistent mineralogy.

A modal analysis on thin section 78236,8B1 (Fig. 1a) revealed a composition of 54 vol.% orthopyroxene (opx) and about 40% plagioclase (plag) (Table 1), which is in good agreement with the mineralogy of 78235 and 78238. Modal abundances of both opx and plag in those samples have been previously reported as 40–60 vol.% (Jackson *et al.*, 1975). Partly devitrified dark-brown mesostasis occurs interstitially—mostly intergranular be-

Table 1. Modal composition of 78236,8.

Phase	Vol. %
Orthopyroxene	53.6
Plagioclase	39.2
Mesostasis	2.4
Clinopyroxene	0.6
Glass	4.0
Accessories	0.2

tween pyroxene grains—and contains tiny clinopyroxene and opaque crystals (~20 μm). At highest magnification the petrographic microscope reveals glassy areas within the mesostasis, which are most probably relics of the residual melt (cf. McCallum *et al.*, 1975; El Goresy *et al.*, 1976). Defocused beam electron microprobe analyses (DFB) showed that the high K and Si contents of the mesostasis are very irregularly distributed (Table 2).

Small amounts of light-green clinopyroxene coexist with orthopyroxene, and from the Fe–Mg partition coefficient of these two phases, a re-equilibration temperature of ~800°C was inferred (McCallum *et al.*, 1975). In addition, less than 0.2 vol.% of accessory phases, such as opaques (chromite, troilite, metallic iron), silica inclusions in plagioclase, whitlockite, apatite, and rutile have been described in all samples, and various amounts of colorless or brownish glass, small veins of which cut the norite along pre-existing grain boundaries and fractures, complete the mode of the Station 8 norite. Carlson and Lugmair (1981) have pointed out the importance of REE-rich accessory phases in 78236 for isotopic equilibration processes. In particular, the small whitlockite content which contains ~10% of the total rock REE abundances due to its very high REE content (up to

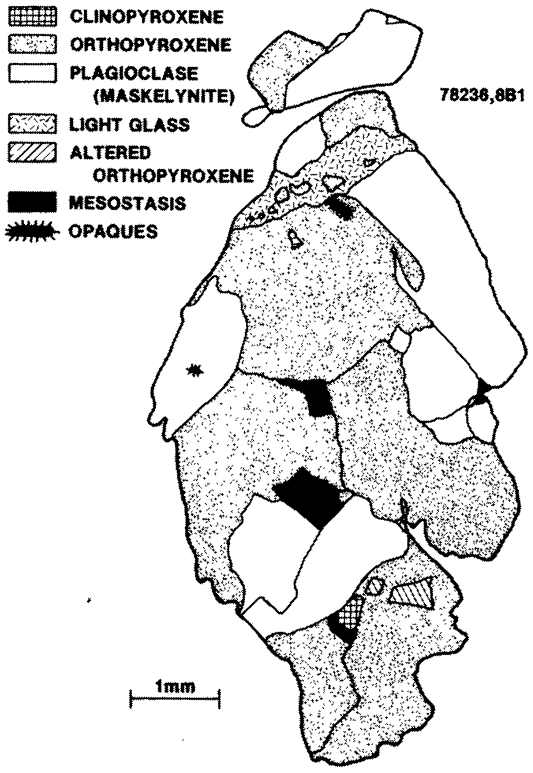

Fig. 1a. Overlay graph of thin section 78236,8B1 showing texture and modal composition of the norite (cf. text).

Fig. 1b. Fragment of 78236,8. A large maskelynite grain with opaque and light euhedral inclusions (cf. text). Adherent fragments of heavily fractured pyroxene with opaque crack fillings. On left and center top areas of light or brown melt showing flow structures (note large vesicle!). Light melt on the left extends into maskelynite, but the light color indicates that this glass must have been formed *in situ* (pure plagioclase composition!); parallel nicols. Width of larger side is 3.2 mm.

Fig. 1c. Same fragment as Fig. 1b, but crossed nicols. Maskelynite shows fibrous devitrification structure and contains core of crystalline plagioclase (center). Melt veins are recrystallized, even the light plagioclase melt-cutting maskelynite.

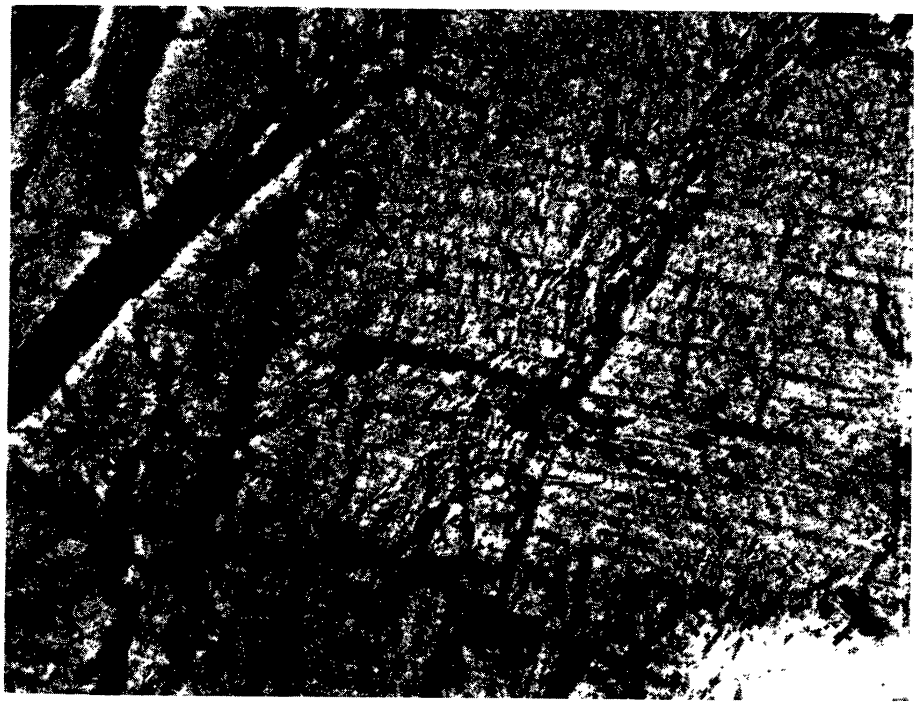

Fig. 1d. Orthopyroxene from 78236,8 displaying multiple sets of planar deformation structures. Note oriented opaque inclusions in the lower half of the picture. This grain is diagonally cut by a zone that experienced high strain resulting in irregular cracks. Parallel nicols, width of larger side is ~300 μm.

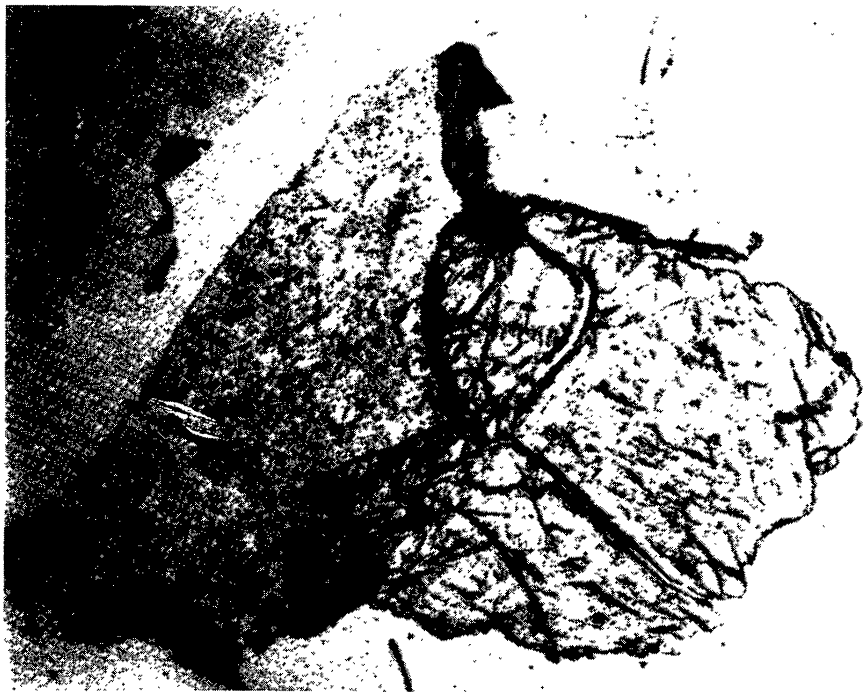

Fig. 1e. Another fragment of 78236,8 composed of densely fractured orthopyroxene and inclusion-rich maskelynite (light). Note dark reaction rims at contact between orthopyroxene and maskelynite, Fe enrichment resulting in the dark (light-brown) color extending into maskelynite. Parallel nicols, width of larger side is 3.2 mm.

1.7% Ce; Winzer *et al.*, 1975; McCallum and Mathez, 1975) must be considered in the interpretation of isotopic data.

In Table 2 we present microprobe analyses of orthopyroxene, plagioclase, glass of various colors, mesostasis, and various types of inclusions in plagioclase. The average compositions of plagioclase ($Ab_3An_{96}Or_1$) and orthopyroxene ($En_{67}Fs_{29}Wo_4$) in 78236 are very similar to those given for 78235 and 78238. Numerous electron microprobe line-scans showed that zoning could not be detected in either plagioclase or orthopyroxene and that the mineral compositions are extremely homogeneous throughout the sample. A few spots of potassium-rich feldspar ($Ab_{2.1}An_{7.1}Or_{90.8}$) were analyzed only along the grain boundaries of two plagioclase grains.

The glass shows a wide compositional range from glass of pure plagioclase chemistry (colorless) to light- and dark-brown melts with increasing amounts of a pyroxene component (Figs. 1b and 1c).

The mesostasis of 78236,8 was analyzed with both a focused and a defocused electron beam (Table 2). Its glassy matrix displays a major element composition very similar to alkali feldspar, and together with some analyses of pure silica this fact leads to the conclusion that these two phases represent the last stage of solidification of the parental liquid of the norite. Reflected light microscopy with high magnification resolved a graphic to myrmekytic intergrowth of silica and glassy matrix. The same texture has been described by Stolper and McSween (1979) in the mesostasis of the Shergotty achondrite. Small inclusions (type B in Table 2) of a similar alkali feldspar composition ($Ab_{16.2}An_{4.2}Or_{79.5}$) have been found in plagioclase grains. They consist of euhedral, $<10\ \mu m$ (rectangular) grains of light-pink color, and are oriented in sets along the (100) plane of the host crystal. Furthermore, some silica-rich inclusions (type A, Table 2) and some $<15\ \mu m$ clinopyroxene grains were found intragranular to plagioclase.

The whole sample displays the deformation features of severe shock metamorphism (Figs. 1c–1e). All orthopyroxene grains show mosaicism, planar deformation structures, and (less abundant) mechanical twinning shock features that are characteristic for a stage I shock metamorphism (Stöffler, 1971). Some pyroxene grains are brecciated at their margins and opaque patches or fracture fillings are abundant and probably due to high temperature decomposition of the pyroxene.

These brecciation zones often grade into regions of partly recrystallized melt that are composed of either light, schlieren-rich glass of plagioclase composition or of brownish, recrystallized glass of approximately pyroxene chemistry (Table 2). Frequently, orthopyroxene clasts are embedded in the melt showing the same degree of shock metamorphism and very often common extinction with adjacent primary pyroxene grains. Also, in thin section 78236,8A1, part of the light glass is recrystallized into rosettes of feldspar crystallites. The brown glass exhibits whisker growth of orthopyroxene (cf. Sclar and Bauer, 1975). All plagioclase grains are at least in part transformed to diaplectic glass (maskelynite) which is now completely devitrified. Most maskelynite grains still contain crystalline cores with planar shock features. Many small inclusions are scattered in maskelynite. They consist of opaque phases which are probably the same composition as the iron rods and metal particles described by Sclar and Bauer (1975, 1976) and Mehta and Goldstein (1980) and which are concentrated in the maskelynized parts of feldspar grains. Some contacts of maskelynite to orthopyroxene grains are outlined by light-brown rims of less than $50\ \mu m$ thickness, evidently indicative of oxidation of Fe^{2+} to Fe^{3+} and elemental exchange between the two mineral phases (Fig. 1).

From the occurrence of diaplectic feldspar glass, the peak shock pressure 78236 experienced is estimated to have been greater than 30 GPa (Stöffler, 1972), but insufficiently high to produce shock-melted plagioclase and pyroxene glass, which would require more than 50 GPa (Schaal *et al.*, 1979). Sclar and Bauer (1975) and El Goresy *et al.* (1976) have already discussed the two possibilities of shock history that may have resulted in the heterogeneous distribution of shock intensities observed in all chips from the norite boulder:

1. A *single stage* impact history in the course of which peak shock pressure and

1982LPSC...12...67N

Table 2. Microprobe analyses of various mineral phases from 78236. Plagioclase and orthopyroxene analyses are averages of a number of analyses. The range of glass composition indicates the variable chemistry of colorless plagioclase glass and light- to dark-brown glass rich in pyroxene component. The analyses of glassy matrix of the mesostasis (focused beam analysis) are accompanied by considerable alkali loss (98 wt.%!). The original data of the defocused beam (DFB) analysis of mesostasis and of the inclusion Type B (in plagioclase) have been recalculated to 100%. Data were obtained by using the MAC microprobe at JSC. Numbers of analyses averaged are given in brackets.

	Plagioclase (4 an.)	1σ	O'pyroxene (4 an.)	1σ	Glass (5 an.) light-dark	Mesostasis (foc. beam)	Mesostasis DFB	Type A Inclusion (5 an.)	1σ	Type B Inclusion
SiO_2	44.70	0.36	53.80	0.19	44.40⇆52.20	75.06	83.85	83.40	1.40	67.71
TiO_2	0.03	0.04	0.30	0.04	0.06⇆ 0.22	—	0.49	0.60	0.30	0.01
Al_2O_3	35.36	0.34	0.90	0.05	35.80⇆18.00	13.24	9.49	7.65	0.80	19.98
FeO	0.02	0.01	12.50	0.36	0.13⇆ 5.54	1.09	0.10	0.05	0.03	—
MgO	0.04	0.03	28.70	0.31	0.32⇆12.13	0.24	0.37	—	—	0.02
CaO	18.92	0.17	1.70	0.03	18.77⇆ 9.98	0.72	4.96	4.00	0.35	2.00
Na_2O	0.60	0.04	0.04	0.04	0.59⇆ 0.25	1.27	0.16	0.22	0.06	0.52
K_2O	0.12	0.09	—	—	0.12⇆ 0.07	6.47	0.58	0.34	0.35	9.76
TOTAL	99.79		97.94		100.20⇆98.39	98.09	100.00	96.30		100.00

post-shock temperature were locally increased by the formation of rarefaction waves along preexisting grain boundaries or fractures as observed in experimentally shock-loaded polycrystalline rocks (e.g., Reimold and Stöffler, 1978) and formed the melt *in situ*.

2. A *two-stage* impact history, in which a second impact event produced veins of intrusive melt and the glass-coating of the boulder which already had been shocked to a moderate degree in the first event.

The variable composition of the melt (Table 2) and the characteristics of orthopyroxene clasts in the melt veins favor the *in situ* development of melt as the result of a single impact (see also Winzer *et al.*, 1975).

Only little information is available on the probable post-shock temperature acquired in noritic rocks shocked to the degree observed in 78236. Estimated post-shock temperatures for a stage II shock metamorphism characterized by maskelynization of feldspar range from ~300°C to 900°C (Stöffler, 1971). The work of Duke (1968) and of Arndt and Gonzales-Cabeza (1981) shows that temperatures in excess of 800°C are required to devitrify maskelynite to the extent that is observed in 78236. If the norite boulder was emplaced into a thick, hot ejecta blanket, this temperature apparently was available for a period of time long enough to recrystallize the maskelynite completely. That the glass coating of the boulder is not recrystallized can be explained by rapid cooling during ballistic transport. Subsequently, a second event must have excavated the boulder to its present position. This stage of the norite history could be consistent with the exposure age of 292 ± 14 m.y. measured by Drozd *et al.* (1977).

Norite 78236 is similar to the Shergotty meteorite with respect to mineralogy and degree of shock metamorphism (shock stage I of pyroxene; transformation of plagioclase into maskelynite; cumulate texture; Duke, 1968; Stolper and McSween, 1979). From papers by Bogard *et al.* (1979) and Nyquist *et al.* (1979b) it is known that the K–Ar, Rb–Sr, and Sm–Nd isotope systems of Shergotty have been reset by a shock event. However, the maskelynite in Shergotty has not been devitrified, providing evidence for a less severe thermal event than 78236 experienced. The heating experiment by Duke (1968) showed that Shergotty could not have been hotter than 400°C for any significant time after formation of maskelynite.

Sample preparation

The characteristics and processing details of the samples analyzed for Rb–Sr and Sm–Nd are given in Table 3. Subsample ,4 (0.77 g) was coarsely crushed and mineral separates of large grain size [Px 1, Mask 1, the ^{39}Ar–^{40}Ar sample, and the INAA plagioclase sample (Blanchard and McKay, 1981)] were handpicked during crushing. The remaining material, >74 μm, was magnetically separated with a Frantz magnetic separator. Plag 1 and 2, and Mask 2 were handpicked from the nonmagnetic fraction. Px 2 and Px 3 were handpicked from the magnetic fraction.

Subsample ,3 was repeatedly crushed and sieved until all material passed through the 100 mesh sieve. The total sample (1.75 g) was coned and quartered and one quarter (0.3 g) was for major element analysis by XRF (Blanchard and McKay, 1981). One quarter was used for magnetic separation and the remainder was set aside for whole rock stock. The whole rock analysis (Table 3) was of this stock. Mask 3, Px 3, Px 4, and a pyroxene sample used for INAA (Blanchard and McKay, 1981) were handpicked from magnetic and non-magnetic separates, respectively. Px 3 was augmented by coarse material from subsample, 3. A small sample of dark-brown glass (DBG) was handpicked from the magnetic and non-magnetic fractions of ,3.

Subsample ,8 (0.67 g) consisted of many coarse fragments handpicked to be free of glass grains prior to allocation. Several of these were selected for INAA analysis (Blanchard and McKay, 1981). Three chips were taken for thin sections—A1, B1, and B2. The remaining material was coarsely crushed and Px 5 and Px 6 handpicked in the same manner as for Px 1.

Comparing our samples to mineral separates described by Carlson and Lugmair (1981), we believe that our Plag 2 most nearly resembles PL-2 and PL-3 of the La Jolla group; our Mask 1 is similar to their PL-4, our Mask 2 to their PL-5, and our Px 2 to their PX-1. Further details of grain size, color, and estimated purity are summarized in Table 3. Grain mounts of several separates were made for petrographic examination.

1982LPSC...12...67N

Table 3. Characteristics of analyzed mineral separates from 78236.

Sample No.	Subsample Number	Sample Processing	Color	Grain Size	Weight (mg)	General Characteristics
Plag 1	78236,4	Handpicking following magnetic separation	Clear-white	>0.05 mm	8.7	Mixture of plag and mask
Plag 2	78236,4	Handpicking following magnetic separation	White	2–0.05 mm	79.9	~70% crystal. plag, ~30% devitrified maskelynite
Mask 1	78236,4	Handpicked from coarsely crushed bulk material	Blue-gray	2–0.15 mm	8.7	
Mask 2	78236,4	Handpicking following magnetic separation	Colorless, glassy	2–0.05 mm	41.2	70–80% mask.; rest is crystal. plag; >95% feldspar
Mask 3	78236,3	Handpicking following magnetic separation	Colorless, glassy	0.15–0.05 mm	23.4	70–80% mask; >95% feldspar
Px 1	78236,4	Handpicked from coarsely crushed bulk material	Light-brown	2–0.15 mm	19.6	>95%
Px 2	78236,4	Handpicking following magnetic separation	Light-brown to yellowish, not translucent	1–0.05 mm	120.2	>95%, inclusions in large grain
Px 3	78236,4	Handpicking following magnetic separation	Same as Px 2	3–<0.1 mm	58.5	>95%
Px 4	78236,3	Handpicked following magnetic separation	Yellowish, not translucent	100–200 mesh	55.5	~95%, some yellowish plagioclase
Px 5	78236,8	Handpicked from coarsely crushed bulk material	Light-brown	3–0.5 mm	55.3	
Px 6	78236,8	Handpicked from coarsely crushed bulk material	Light-brown	3–0.5 mm	70.9	
DBG	78236,3	Handpicked from magnetic and nonmagnetic separates	Dark-brown	0.15–0.05 mm	3.3	~70% dark glass, rest dark-brown pyroxene and 10% plagioclase
WR	78236,3	Aliquant of single 1.75 g chunk		<0.15 mm	35.3	

ISOTOPIC ANALYSES

Rb–Sr and Sm–Nd analytical procedures

Ion exchange column procedures used for Plag 1 and 2, Mask 1 and 2, and Px 1 and 2 were similar to those previously used in our laboratory (Gast *et al.*, 1970; Nyquist *et al.*, 1979a). Rb and Sr blanks for this procedure were typically ~0.05 ng Rb and ~1 ng Sr. However, Sr blanks run after the 80 mg Plag 2 sample were ~10 ng. We determined that the high blank was memory from the previously analyzed sample. Apparently the 0.1 M oxalic acid used in this technique causes a small amount of Ca^{++} to precipitate and remain on the column when large plagioclase samples are processed. The analysis sequence had been such that this problem did not affect any of the prior analyses. Most of the later samples were processed with a modified procedure in which no oxalic acid is used but the alkalis are first eluted with 0.6 N HBr as before. Further elution is with 2.0 N HCl. Blanks for this procedure are typically ~0.03 ng Rb and ~0.3 ng Sr with no Sr memory. Although the 0.6 N HBr usually yields very clean separations of the alkalis, the high Fe and Mg content of 78236 pyroxenes required that Rb fractions from ~50 mg samples be further purified prior to analysis. This was done by a second HBr elution through smaller columns with Rb blanks of ~0.02 ng. The second elution was necessary for Px 3, 4, 5, and 6, but was not used for other samples. Prior to adoption of our final techniques, an interim procedure involving only elution with 1.5 N HCl was used for Mask 3 and Px 3. This procedure was found to be satisfactory for plagioclase, but the large amount of Fe in the Rb fraction of Px 3 resulted in the loss of that analysis.

Sm–Nd procedures were the same as previously described (Nyquist *et al.*, 1979a) and were unaffected by the problems encountered for Rb–Sr. Blanks remained constant at ~0.025 ng Sm and ~0.15 ng Nd, respectively. Blanks of spike solutions and chemical reagents were negligible compared to the total blank values throughout the entire sample processing. Separation of Sm from Nd was good with $^{144}Sm/^{144}Nd < 10^{-5}$ (as inferred from $^{147}Sm/^{144}Nd$) with the exception of the Px 2 analysis (Table 5).

The first suite of samples (Plag 1, Mask 1, Px 1) was spiked for K, Rb, and Sr. The dark-brown glass was spiked only for Rb and Sr. All other samples were spiked for Rb, Sr, Sm, and Nd.

Mass spectrometric procedures have been described previously (Nyquist *et al.*, 1979a). Eight analyses of NBS 987 performed during the course of this investigation yielded an average normalized $^{87}Sr/^{86}Sr = 0.71021 \pm 3$. Four analyses of our Ames Nd metal standard during this investigation yielded an average $^{143}Nd/^{144}Nd = 0.511146 \pm 28$ normalized to $^{148}Nd/^{144}Nd = 0.24308$. A single analysis of the La Jolla Nd_2O_3 standard gave normalized $^{143}Nd/^{144}Nd = 0.511116 \pm 33$. These results are in satisfactory agreement with our earlier values for these standards (Nyquist *et al.*, 1979a). An average $^{145}Nd/^{144}Nd = 0.34897 \pm 3$ was measured for the 78236 samples. The good agreement with $^{145}Nd/^{144}Nd$ results for isotopic standards shows that spike corrections were adequate and that there are no undetected interferences.

K, Rb, and Sr results

K, Rb, and Sr analytical results are reported in Table 4, and Rb–Sr isotopic data are plotted in Fig. 2. The Sr content of the five plagioclase samples is remarkably constant with an average value of 208 ± 2 ppm, exactly twice that measured for the whole rock sample. The Sr content of the pyroxene separates is about two orders of magnitude lower. These observations are consistent with the homogeneity of the plagioclase/maskelynite as found during the electron microprobe analyses and with a modal composition of ~50% plag. They imply that there are no additional reservoirs which contribute substantially to the Sr budget. The Rb and Sr contents of our dark-brown glass (DBG) sample are nearly identical with those of the whole-rock sample. This observation strongly favors our interpretation of the glass genesis, i.e., *in situ* production of norite melt. Rb contents of plagioclase samples are considerably more variable than the Sr contents, suggesting the presence of variable amounts of alkali-rich type B inclusions and/or the presence of mesostasis. The K-content of these inclusions (Table 2) is about two orders of magnitude higher than that of plagioclase, so an estimated maximum abundance of ~0.1% would be expected to contribute ≲10% of the K, Rb inventory. This conclusion is supported by the ^{39}Ar–^{40}Ar analysis which shows a constant K/Ca ratio of 0.006–0.007 over 97% of the ^{39}Ar released.

There is a fourfold variation in Sr and a nearly threefold variation in Rb concentrations among the pyroxene separates, suggesting significant contributions of trace contaminating phases. The mesostasis is the most probable contributor to the Rb inventory. Less than 1% of mesostasis of the type analyzed by DFB (Table 2) could contribute the entire K

Table 4. K, Rb, and Sr analytical results for 78236.

Sample	wt. (mg)	K (ppm)	Rb (ppm)	Sr (ppm)	$\frac{^{87}Rb}{^{86}Sr}$ [(a)]	$\frac{^{87}Sr}{^{86}Sr}$ [(b)]
WR[(c)]	35.3	—	0.862	104.0	0.02398 ± 17	0.70057 ± 4
Plag 1[(d)]	8.7	844	1.056	207.1	0.01475 ± 11	0.70005 ± 6
Plag 2[(d)]	79.9	—	1.168	206.9	0.01634 ± 12	0.70011 ± 5
Mask 1[(d)]	8.7	789	0.796	209.9	0.01097 ± 8	0.69979 ± 7
Mask 2[(d)]	41.2	—	0.966	206.5	0.01354 ± 10	0.70003 ± 5
Mask 3[(e)]	23.4	—	1.450	210.3	0.01995 ± 15	0.70030 ± 5
Px 1[(d)]	19.6	42.6	0.237	1.56	0.44	—
Px 2[(d)]	120.2	—	0.195	2.42	0.233 ± 2	0.71282 ± 8
Px 3[(e)]	58.5	—	0.25[(g)]	2.03	—	0.72135 ± 9
Px 4[(c)]	55.5	—	0.259	6.20	0.1208 ± 9	0.70531 ± 6
Px 5[(c)]	55.3	—	0.407	2.32	0.508 ± 4	0.73095 ± 8
Px 6[(c)]	70.9	—	0.526	4.86	0.313 ± 3	0.72176 ± 5
DBG[(c)]	3.3	—	0.956	99.06	0.0279 ± 2	0.70069 ± 6
NBS 987[(f)]						0.71021 ± 3

(a) Uncertainties correspond to last figures.
(b) Uncertainties correspond to last figures and are $2\sigma_m$. Normalized to $^{88}Sr/^{86}Sr = 8.37521$.
(c) Final Rb–Sr procedure.
(d) Initial Rb–Sr procedure.
(e) Interim Rb–Sr procedure.
(f) Average of 8 analyses from April, 1980 to April, 1981.
(g) Rb content calculated assuming a 4.3 AE age.

inventory of Px 1. Mesostasis contamination at the percent level seems easily possible, particularly as mesostasis often is poikilitically intergrown with pyroxene (Fig. 1b). Variations in Sr contents are not closely correlated to variations in Rb contents, suggesting the presence of more than one trace phase in the pyroxene separates. Plagioclase and mesostasis containing whitlockite are candidates for the Sr-bearing phase. About 1% of plagioclase would contribute about 2 ppm of Sr. However, as discussed more fully later, the "excess" Sr in Px 4 and Px 6 must have an isotopic composition differing from that in plagioclase.

In spite of the susceptibility of pyroxene to Rb and Sr contributions from contaminating phases, four of the six pyroxene analyses have Rb in the range 0.20–0.26 ppm, a 30% variation; and four of six Sr analyses are in the range 1.6–2.4 ppm, a 50% variation. Thus, we expect that the Rb and Sr inventory of these samples is not dominated by mesostasis because of the very sensitivity of Rb contents to variable amounts of mesostasis contamination. This conclusion is supported by an analysis by Blanchard and McKay (1981) who found the typical LREE depleted orthopyroxene REE abundance pattern for a pyroxene separate similar to ones which we analyzed. In contrast, McCallum and Mathez (1975) report REE abundances which are severely LREE enriched in whitlockite contained in mesostasis "restricted to interstitial areas" and making up 0.012 vol.% of the 78236 mode. REE abundances in pyroxene should be very sensitive to whitlockite contamination because abundances in whitlockite are $\sim 10^4$ higher than in pyroxene. The generally high Sm/Nd ratios of our pyroxene separates imply little or no whitlockite contamination. This is particularly true of Px 2 which was painstakingly handpicked from material of fine grain size in order to avoid dark mesostasis and select only orthopyroxene. This sample also has the lowest Rb content. There is some possibility of maskelynite contamination of this sample because of the difficulty of distinguishing between light-brown pyroxene and some yellowish maskelynite. We thus believe the intrinsic Rb and Sr contents of 78236 orthopyroxene to be ~ 0.2 ppm and ~ 1.6–2 ppm, respectively.

The $^{87}Sr/^{86}Sr$ ratios of plagioclase, maskelynite, and whole rock are closely correlated

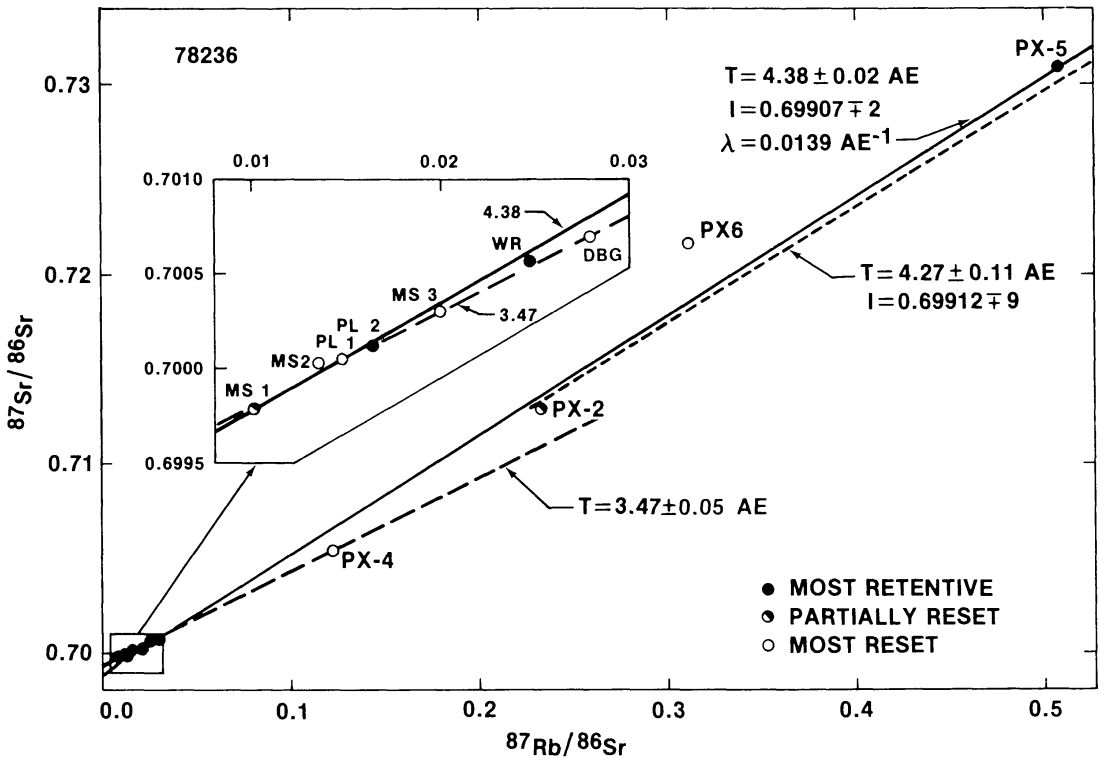

Fig. 2. Rb–Sr data for mineral separates from shocked lunar norite 78236. Error limits are smaller than symbol size. The data have been classified as (i) most retentive, (ii) partially reset, and (iii) most reset by comparison of Rb–Sr and Sm–Nd isotopic data and by petrographic observations (see text). Whole rock (WR), plagioclase (PL), dark-brown glass (DBG), and maskelynite (MS) data are shown in the inset. The pyroxene (PX) data control values of apparent ages. A linear regression (York, 1966) to the most retentive data yields an apparent age $T = 4.38 \pm 0.02$ AE and initial $^{87}Sr/^{86}Sr$ $I(Sr) = 0.69907 \mp 2$ for $\lambda(^{87}Rb) = 0.0139\ AE^{-1}$ and 2σ error limits. A linear regression including partially reset PX 2 and MS 1 yields $T = 4.27 \pm 0.11$ AE, $I = 0.69912 \mp 9$. A linear regression to the four most reset data (MS 2, MS 3, DBG, PX 4) yields $T = 3.47 \pm 0.05$ AE as an upper limit for the age of the last event to affect the Rb–Sr system. For $\lambda(^{87}Rb) = 0.0142\ AE^{-1}$ (Steiger and Jaeger, 1977), the above ages are 4.29, 4.18, and 3.40 AE, respectively.

to the $^{87}Rb/^{86}Sr$ ratios (Fig. 2), whereas the pyroxene data scatter considerably. Px 4 and Px 6 are most aberrant. A tie line between Px 4 and the whole rock datum yields an apparent age of 3.44 AE. This is an upper limit to the time of occurrence of the most recent event affecting the Rb–Sr system if the whole rock sample is representative of the bulk system. The model age of Px 4 relative to LUNI = 0.69903 is 3.67 AE (Table 6) and is a rigorous but less restrictive upper limit. The difference between the LUNI model age of Px 4 and its model age relative to the whole rock analysis is small, showing that the latter is insensitive to sampling inhomogeneities. Thus, because of the care taken to ensure that the whole rock analysis was representative, the ~3.44 AE age can be considered a safe upper limit for the last event. We identify the ≲3.44 AE event with the time of shock metamorphism during which maskelynite and shock glass were produced in 78236. Combining Px 4 and dark-brown glass (DBG) with Mask 2 and Mask 3 yields an isochron of apparent age of 3.47 ± 0.05 AE as shown in the figure. Of the feldspar samples, Mask 2 and Mask 3 are most likely to have undergone isotopic re-equilibration with other phases during post-shock thermal annealing. Because the glass (DBG) was a completely molten phase of 78236, it is also apt to have been isotopically re-equilibrated following the shock event. As our analyses of the four most reset mineral separates yield a well defined isochron, we tentatively ascribe time significance to this isochron and suggest that 78236 was shock metamorphosed ~3.47 AE ago.

The other aberrant datum, Px 6, is displaced towards unacceptably high ages and contains no age information. Note that both Px 4 and Px 6 have Sr contents about

threefold greater than the ~2 ppm which we believe to be intrinsic to pyroxene. We cannot identify the contaminant phase uniquely, but note that it cannot be simply feldspar of the type analyzed, since addition of such a contaminant would simply cause the data to lie along a single mixing line between plagioclase and pyroxene end members. The light-brown contact zones between some opx and maskelynite grains show evidence of elemental exchange between these minerals (see petrography section and Fig. 1) and could be a source of anomalous Sr. At any rate, we classify Px 4 and Px 6 as among the most disturbed samples analyzed and exclude them from any consideration of the crystallization age of 78236.

When Px 4 and Px 6 are excluded, the remaining data define an isochron of age $T = 4.27 \pm 0.11$ AE and initial $^{87}Sr/^{86}Sr\ I = 0.69912 \mp 9$. The age is controlled by Px 5 and Px 2, both of which lie off the isochron by more than analytical uncertainty. Comparison of Rb–Sr and Sm–Nd data, discussed below, indicates that Px 5 has remained a closed system. Thus, in Fig. 2 we also show a 4.38 ± 0.02 AE isochron through Px 5, the whole rock, and the feldspar data.

Sm isotopic composition and neutron exposure

The following isotopic ratios were measured for an unspiked whole rock sample of 78236,3: $^{147}Sm/^{152}Sm = 0.56081$ (normalization); $^{148}Sm/^{152}Sm = 0.42041 \pm 4$; $^{149}Sm/^{152}Sm = 0.51538 \pm 2$; and $^{150}Sm/^{152}Sm = 0.27741 \pm 5$ (uncertainties are $2\sigma_m$). Whereas normalized $^{148}Sm/^{152}Sm$ is within error limits of the value obtained for terrestrial standards, $^{149}Sm/^{152}Sm$ is depleted and $^{150}Sm/^{152}Sm$ enhanced due to neutron capture on ^{149}Sm. The $^{150}Sm/^{149}Sm = 0.53826 \pm 10$ which may be compared to a terrestrial value between 0.53403 ± 5 (Russ *et al.*, 1971) and 0.53406 ± 5 (Lugmair *et al.*, 1975, and unpubl. JSC data). Furthermore, our 78236 data fall on the $^{150}Sm/^{152}Sm$ versus $^{149}Sm/^{152}Sm$ correlation for lunar samples (Russ *et al.*, 1971; Curtis and Wasserburg, 1975). Following Russ *et al.* (1971) we define

$$\epsilon_{Sm} = \frac{(^{150}Sm/^{149}Sm)_m - (^{150}Sm/^{149}Sm)_o}{1 + (^{150}Sm/^{149}Sm)_m}$$

where subscripts "m" and "o" denote measured and original (terrestrial) values, respectively. Thus $\epsilon_{Sm} = 0.00275 \pm 8$ n at^{-1} (neutrons/atom). Following Lingenfelter *et al.* (1972), we calculate $\Sigma_{eff} = 2 \times 10^{-3}$ for the major and trace element composition of 78236. This value is considerably lower than typical values of $\Sigma_{eff} \approx 8 \times 10^{-3}$ for lunar regolith samples and introduces a significant uncertainty into the calculation of the neutron fluence and neutron exposure ages. From Fig. 6 of Lingenfelter *et al.* (1972) we find the maximum neutron capture rate at a shielding depth of 150 g/cm^2 to be $\approx 2 \times 10^{-2}$ n at^{-1} AE^{-1} for $\Sigma_{eff} = 2 \times 10^{-3}$ and $\approx 4 \times 10^{-3}$ n at^{-1} AE^{-1} for $\Sigma_{eff} = 8 \times 10^{-3}$. The minimum neutron exposure age is thus only loosely constrained to be in the interval 138–690 m.y., which is consistent with the ^{81}Kr–Kr exposure age of 292 ± 14 m.y. (Drozd *et al.*, 1977). From Fig. 11 of Curtis and Wasserburg (1975), we estimate the effective neutron capture cross section, σ_{eff}, for ^{149}Sm to be $\approx 6 \times 10^4$ barns. The neutron fluence, $\epsilon_{Sm}/\sigma_{eff}$, is thus calculated to be 4.6×10^{-16} n/cm^2; which is in the range of those for Apollo 17 soils (Curtis and Wasserburg, 1975).

The comparatively large neutron effect on ^{149}Sm changes the calculated Sm concentrations by 0.6–1.6% from the previously reported values (Nyquist *et al.*, 1981) which were calculated for a terrestrial isotopic composition. Those values should be disregarded in favor of the values reported in this paper which have been calculated with the measured Sm composition.

Sm and Nd results

Sm and Nd analytical results are reported in Table 5 and plotted on an isochron diagram in Fig. 3. The data are qualitatively similar to those reported by Carlson and Lugmair

Table 5. Sm and Nd analytical results for 78236.

Sample	wt. (mg)	Sm[(a)] (ppm)	Nd (ppm)	$^{147}Sm/^{144}Nd$[(b)]	$^{143}Nd/^{144}Nd$[(c)]	$^{145}Nd/^{144}Nd$	$^{144}Sm/^{144}Nd$[(d)] ($\times 10^{-5}$)
WR	35.3	2.001	7.020	0.1724 ± 2	0.511191 ± 29	0.34896 ± 3	0.8
Plag 2	79.9	1.640	6.811	0.1456 ± 2	0.510363 ± 18	0.34897 ± 5	0.5
Mask 2	41.2	1.122	4.697	0.1445 ± 2	0.510334 ± 39	0.34894 ± 4	0.2
Mask 3	23.4	1.400	6.050	0.1399 ± 2	0.510354 ± 34	0.34897 ± 5	0.2
Px 2	120.2	0.9361	1.526	0.3710 ± 4	0.516731 ± 85	0.34890 ± 10	7.2
Px 3	58.5	0.9211	1.552	0.3589 ± 4	0.516475 ± 36	0.34902 ± 4	0.8
Px 4	55.5	1.027	2.329	0.2667 ± 3	0.513883 ± 21	0.34898 ± 4	0.2
Px 5	55.3	0.9783	2.026	0.2920 ± 3	0.514678 ± 18	0.34900 ± 3	0.4
Px 6	70.9	0.9800	2.228	0.2660 ± 3	0.513738 ± 31	0.34902 ± 4	0.3
Ames Nd[(e)]					0.511146 ± 28	0.34898 ± 3	
La Jolla Nd[(f)]					0.511116 ± 33	0.34893 ± 3	

(a) Calculated using measured Sm isotopic composition.
(b) Uncertainties correspond to last figures and do not include the $\leq 0.1\%$ uncertainty in the Sm/Nd ratio of the spike.
(c) Uncertainties are $2\sigma_m$ and correspond to last figures. Normalized to $^{148}Nd/^{144}Nd = 0.24308$.
(d) Estimated assuming mass 147 due entirely to ^{147}Sm.
(e) Average of 4 analyses for January, 1980 to July, 1980.
(f) Single analysis—January, 1981.

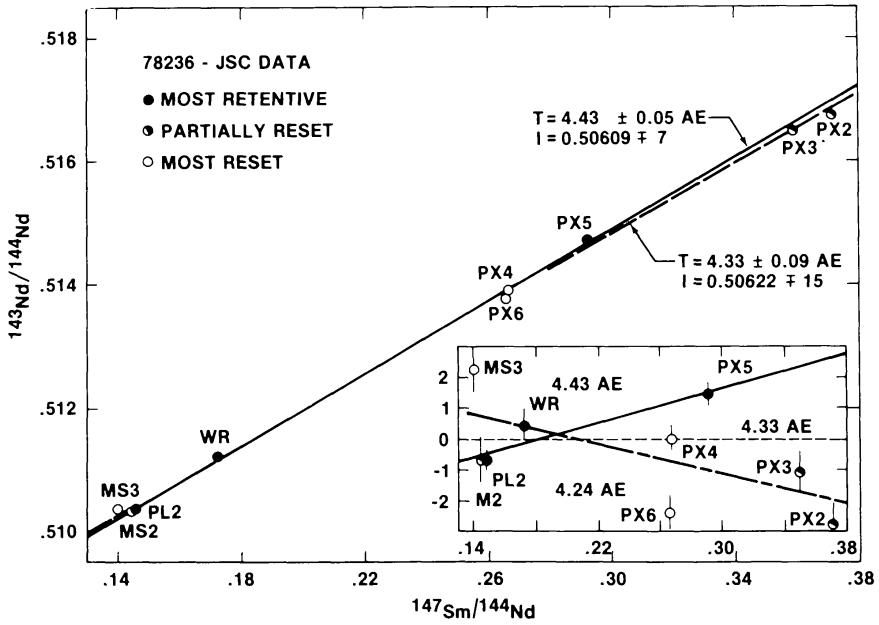

Fig. 3. Sm–Nd data for mineral separates from 78236. Error limits in the main figure are smaller than symbol size. See Fig. 2 for nomenclature. A linear regression to the most retentive data yields an age $T = 4.43 \pm 0.05$ AE and initial $^{143}Nd/^{144}Nd$ $I(Nd) = 0.50609 \mp 7$ for $\lambda(^{147}Sm) = 0.00654$ AE^{-1} and 2σ error limits. A linear regression to all the data yields $T = 4.33 \pm 0.09$ AE and $I(Nd) = 0.50622 \mp 15$. The inset shows the deviation of data from this average isochron in parts in 10^4. Isochrons for the most retentive (PL 2, WR, PX 5) and less retentive (MS 2, MS 3, WR, PX 2, PX 3, PX 4, PX 6) phases are also shown in the inset. The significance of the apparent age of 4.24 AE for the less retentive phases is unclear; however, the Sm–Nd data of Carlson and Lugmair (1980) also show some data aligned on an ~4.20 AE isochron.

(1981). Nd contents of feldspar samples vary from 4.7 to 6.8 ppm and that of pyroxene samples from 1.5 to 2.3 ppm, whereas the whole rock contains 7 ppm Nd. Since the whole rock contains approximately equal amounts of feldspar and pyroxene, it is clear that it must contain phases other than those separated which contribute about 50% of the total Sm and Nd budget. These unseparated phases include mesostasis containing whitlockite; and whitlockite has been estimated by McCallum and Mathez (1975) to contain ~10% of the REE in 78236. It is possible that pyroxene separates with more than 2 ppm Nd contain some whitlockite also. McCallum and Mathez (1975) report Nd and Sm concentrations in whitlockite of 2.35 and 1.81%, respectively. The corresponding $^{147}Sm/^{144}Nd = 0.15$ is consistent with the overall REE abundance pattern reported by these authors and with previous measurements of $^{147}Sm/^{144}Nd$ in meteoritic whitlockites (Lugmair and Marti, 1977; Shih *et al.*, 1981). If Px 2 represents a pure orthopyroxene end member, then equal contributions from pyroxene and whitlockite to the Nd content of a sample will result in $^{147}Sm/^{144}Nd \approx 0.26$. Px 4 and Px 6 fit this description well, especially if the intrinsic Nd content of pyroxene is ~1.2 ppm as found by Carlson and Lugmair (1981) for their PX-4. Comparison of our pyroxene data to their PX-4 suggests that even our Px 2 and Px 3 samples may have a small Nd contribution from whitlockite. Mass balance calculations indicate that if true pyroxene Nd with $^{147}Sm/^{144}Nd = 0.397$ (from La Jolla PX-4) is mixing with whitlockite Nd with $^{147}Sm/^{144}Nd = 0.15$, then ~10, 15, 53, 42, and 53% of the Nd in Px 2, 3, 4, 5, and 6, respectively, is contributed by whitlockite. Similar percentages would be calculated if the "excess" Nd contribution would be from plagioclase contamination, but our pyroxene separates contained considerably less than 10% of identifiable contaminants such as plagioclase. Of course, the possibility that the variable REE content of our pyroxene separates is due to a combination of contributions from both whitlockite and plagioclase cannot be excluded.

A linear regression of all the data in Fig. 3 yields an isochron of apparent age $T = 4.33 \pm 0.09$ AE and initial $^{143}Nd/^{144}Nd = 0.50622 \mp 15$. However, the data scatter about this isochron by considerably more than the error limits as shown by the inset to Fig. 3. These results are very similar to those reported by Carlson and Lugmair (1981). Those authors did not state a formal error limit on their isochron ages because their data, like our own, scattered about the regression line by more than analytical uncertainty. In order to compare the La Jolla and JSC data directly, we regressed their data with the York (1966) program and obtained $T = 4.33 \pm 0.04$ AE. After renormalization to $^{148}Nd/^{144}Nd = 0.24308$ and correcting for the instrument modification discussed by Lugmair and Carlson (1979), the corresponding initial ratio $I(Nd) = 0.50624 \mp 6$. Thus, the data from the two laboratories appear consistent and both data sets show evidence of isotopic disturbance of the Sm–Nd system. Disturbances in the Sm–Nd system are smaller in magnitude than the corresponding disturbances in the Rb–Sr system.

The ages calculated from both Rb–Sr and Sm–Nd measurements are controlled by data for pyroxene separates. It is instructive to compare apparent ages calculated from pyroxene-whole rock tie lines for the two data sets. If the whole rock sample is representative of the bulk rock, it must lie on the isochron for the crystallization age if the bulk rock has remained a closed system. Although the presence of glass veins in 78236 suggests the possibility of incorporation of exterior material into the bulk sample, our petrographic study shows this not to have been the case. Furthermore, the Rb–Sr analysis of the glass was very similar to that of the whole rock. Thus, we consider the assumption that the bulk rock is a closed system is justified. Ages corresponding to pyroxene-whole rock tie lines are given in Table 6 together with the Sr and Nd concentrations in the pyroxene separates. Only the Px 5 ages can be said to be definitely concordant in the two systems. The Px 2 data can be considered concordant within error limits for $\lambda(^{87}Rb) = 0.0139\ AE^{-1}$ but not for $\lambda(^{87}Rb) = 0.0142\ AE^{-1}$. We note that our Rb–Sr and Sm–Nd ages customarily yield better concordance for $\lambda(^{87}Rb) = 0.0139$ than for $\lambda(^{87}Rb) = 0.0142$, so that there is some justification for considering the ages of Px 2 to be concordant within error limits. However, we note that even then the concordancy is at the extreme error limit and so we consider the Px 2 Rb–Sr data as probably partially

Table 6. Ages corresponding to PX-WR tie lines and LUNI model ages for analyzed pyroxene separates.

Sample	T (Sr)	T (Nd)	ΔT	Sr (ppm)	Nd (ppm)	T_L[a]
PX2	4.10 ± 0.08	4.21 ± 0.10	0.11 ± 0.13	2.42	1.53	4.15
	(4.01 ± 0.08)[b]		(0.20 ± 0.13)			
PX3	—	4.27 ± 0.07	—	2.03	1.55	—
PX4	3.44 ± 0.11	4.30 ± 0.11	0.86 ± 0.16	6.20	2.33	3.67
	(3.37 ± 0.11)		(0.93 ± 0.16)			
PX5	4.38 ± 0.04	4.39 ± 0.08	0.01 ± 0.09	2.32	2.03	4.39
	(4.29 ± 0.04)		(0.10 ± 0.09)			
PX6	5.09 ± 0.07	4.11 ± 0.11	−0.98 ± 0.13	4.86	2.23	5.06

(a) T_L = LUNI model age, calculated with $I_L = 0.69903$.
(b) Values in parentheses are calculated for $\lambda(^{87}Rb) = 0.0142\ AE^{-1}$.

reset. We thus conclude that of all the pyroxene samples analyzed, probably only Px 5 predominantly contained material which remained closed to Sr and Nd isotopic equilibration and/or elemental exchange *since the formation of 78236.* If so, the Sr and Nd tie line ages of 4.38 ± 0.04 and 4.39 ± 0.08 AE, respectively, give the crystallization age of the norite within the stated error limits.

By considering the isotopic data and our petrographic observations, we have classified all the mineral separates analyzed for Rb–Sr and Sm–Nd into three categories, i.e., (i) most retentive: Px 5, WR, and PL 1,2; (ii) partially reset: Px 2, Px 3, MS 1; (iii) most reset: Px 4, Px 6, MS 2, MS 3, DBG. Linear regressions to the most retentive minerals give T(Sr) = 4.38 ± 0.02 AE, I(Sr) = 0.69907 ∓ 2 and T(Nd) = 4.43 ± 0.05 AE, I(Nd) = 0.50609 ∓ 7. Making a similar categorization of the La Jolla Nd data gives T(Nd) = 4.38 ± 0.01 AE, I(Nd) = 0.50618 ∓ 2. In the latter case we consider the error limits as fortuitously small, since the regressed data (PL-4, PL-5, Px-2) essentially define a "two-point" line. We further note that Carlson and Lugmair chose to use the totally spiked data of Px-2. The unspiked Px-2 analysis would yield T(Nd) = 4.48 AE (Carlson and Lugmair, 1980). We do not consider the ~4.4 AE ages fortuitious, particularly as there is support for this age in the ^{39}Ar–^{40}Ar data. Thus, we currently consider the best value of the crystallization age of 78236 to be 4.43 ± 0.05 AE as obtained from the Sm–Nd analyses of the most retentive samples. We discuss the implications of this age, probable causes of isotopic disturbances, and some alternate interpretations after presentation of the ^{39}Ar–^{40}Ar data.

^{39}Ar–^{40}Ar analyses

A 50.4 mg sample of coarse-grained feldspar similar to Mask 1 in Table 3 was handpicked from subsample 78236,4 for ^{39}Ar–^{40}Ar analysis. The sample was irradiated with $\sim 2 \times 10^{18}$ fast neutrons, then heated in a high vacuum furnace in a series of increasing temperature steps. The isotopic composition of the released Ar was measured on a mass spectrometer. Hornblende fluence monitors irradiated with the feldspar sample gave ^{39}Ar–^{40}Ar ratios of 0.0307 ± 0.0004 and 0.0313 ± 0.0004. Details of the experimental procedure and of the data calculations are given in Bogard *et al.* (1976). Measured argon isotopic data are given in Table 7. ^{39}Ar–^{40}Ar ages were calculated for each temperature step using the constants recommended by Steiger and Jäger (1977) and are presented as a function of ^{39}Ar release in Fig. 4.

The feldspar sample from 78236,4 was much more retentive of its argon than other meteoritic, lunar, and terrestrial feldspars (including maskelynite and plagioclase of high An content) which we have previously analyzed. The 78236,4 sample released over 60% of its ^{39}Ar at temperatures in excess of 1200°C. The highest extraction temperature of 1625°C is higher than the predicted melting point of ~1540°C for plagioclase of An ~96.

1982LPSC...12...67N

Table 7. Argon isotopic data for the stepwise temperature release of 78236,4 feldspar. Corrections were made for system blanks and reactor-produced interferences. Uncertainties in isotope ratios are derived from measurement uncertainties, blank corrections, and the uncertainties in applied reactor corrections. Absolute concentrations of ^{39}Ar are ±10%. Ages were calculated using the K decay parameters given by Steiger and Jäger (1977).

Temp. °C	$^{39}Ar\ 10^{-8}\ cm^3$ STP/g	$^{40}Ar/^{39}Ar$	$^{38}Ar/^{39}Ar$	$^{37}Ar/^{39}Ar$	$^{36}Ar/^{39}Ar$	K/Ca	Age 10^9 yr
300	0.39	48.5 ± 17.4	0.96 ± 0.52	0.24 ± 0.17	1.5 ± 0.8	2.1 ± 1.5	3.2 ± 0.5
450	0.13	1277 ± 5	0.65 ± 0.86	13.9 ± 0.5	0.27 ± 0.21	0.037 ± 0.001	8.8 ± 0.1
550	0.12	144.6 ± 4.0	0.56 ± 0.09	34.4 ± 2.0	0.59 ± 0.19	0.015 ± 0.001	4.98 ± 0.05
650	0.17	91.0 ± 3.0	0.27 ± 0.08	35.4 ± 1.6	0.36 ± 0.14	0.0145 ± 0.0007	4.22 ± 0.06
750	0.55	31.9 ± 0.7	0.300 ± 0.024	33.1 ± 1.0	0.49 ± 0.05	0.0150 ± 0.0005	2.62 ± 0.04
850	0.60	58.2 ± 1.5	0.680 ± 0.027	70.9 ± 2.5	0.85 ± 0.05	0.0072 ± 0.0003	3.50 ± 0.04
950	0.91	26.4 ± 0.7	0.692 ± 0.028	77.4 ± 4.2	0.772 ± 0.022	0.0066 ± 0.0004	2.36 ± 0.04
1100	4.51	70.0 ± 1.2	0.710 ± 0.015	83.3 ± 1.7	0.581 ± 0.012	0.0061 ± 0.0001	3.79 ± 0.03
1200	9.39	89.7 ± 1.0	0.692 ± 0.011	83.4 ± 1.3	0.485 ± 0.008	0.0061 ± 0.0001	4.19 ± 0.03
1300	9.99	95.1 ± 1.1	0.694 ± 0.009	83.4 ± 1.3	0.473 ± 0.010	0.0061 ± 0.0001	4.29 ± 0.03
1450	4.08	112.4 ± 1.6	0.706 ± 0.012	84.4 ± 1.5	0.500 ± 0.044	0.0061 ± 0.0001	4.56 ± 0.03
1600	11.26	101.7 ± 1.1	0.692 ± 0.010	83.4 ± 1.3	0.477 ± 0.020	0.0061 ± 0.0001	4.40 ± 0.03
1625	3.67	146.3 ± 2.2	0.710 ± 0.016	83.0 ± 1.6	0.570 ± 0.052	0.0062 ± 0.0001	5.00 ± 0.04

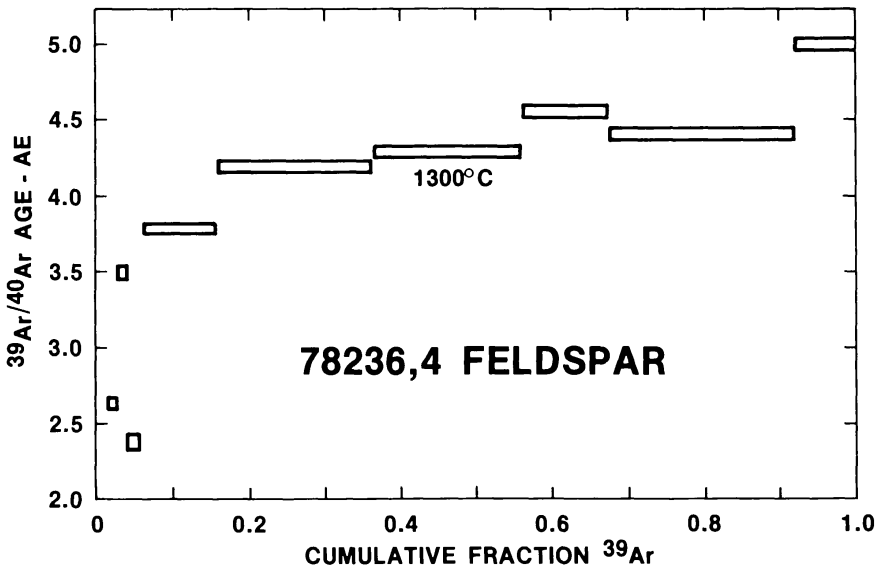

Fig. 4. $^{39}Ar/^{40}Ar$ ages as a function of ^{39}Ar released during stepwise degassing of a feldspar separate from 78236,4. The midpoint of the ^{39}Ar release occurred at 1300°C.

Nevertheless, our maskelynite sample may not have been completely degassed of its Ar. The calculated K and Ca concentrations in our sample of 0.062% and 9.2%, respectively, are about 20–30% lower than concentrations listed in Tables 2 and 4. Our sample, therefore, may have been degassed of only ~70–80% of its argon. Any undegassed Ar would likely show ^{39}Ar–^{40}Ar ages at least as large as those extractions ≥1300°C and should not substantially affect our conclusions on the K–Ar age.

The ^{39}Ar–^{40}Ar age quickly rises to a value of 4.2 AE between 2% and 16% of the ^{39}Ar released (650°C through 1100°C), then slowly increases with increasing extraction temperature (Fig. 4). Extractions from 300°C through 650°C released only very small amounts of Ar and probably contained small, variable amounts of atmospheric Ar. Thus, we attach no significance to the high ages for these low temperature extractions. Extractions from 850°C through 1625°C showed constant K/Ca ratios, whereas extractions from 450°C through 750°C (releasing only ~3% of the ^{39}Ar) showed somewhat higher K/Ca ratios. This behavior of the K/Ca is consistent with plagioclase of uniform composition releasing most of the Ar, but with small amounts of alkali-enriched feldspar or glass releasing Ar at lower temperatures. The high ^{39}Ar–^{40}Ar age for the 1625°C extraction does not appear to be due to atmospheric Ar, as the blank correction is small and the $^{36}Ar/^{37}Ar$ ratio is similar to previous extractions. The anomalously high age for the 1625°C extraction may be due to radiogenic ^{40}Ar redistributed by the shock event which formed the maskelynite, or to recoil effects produced in the reactor.

The average ^{39}Ar–^{40}Ar age for all temperature releases of 78236,4 feldspar is 4.26 AE; the average age for extraction temperatures of 1100°C and above (with 94% of the ^{39}Ar release) is 4.33 AE. The former age would be a lower limit for either the crystallization age or the time of last major Ar degassing of 78236. The ^{39}Ar–^{40}Ar data permit the crystallization age to be older than ~4.3 AE, however, as inferred from the Rb–Sr and Sm–Nd studies. For example, under the assumption that some ^{40}Ar has been lost from lower temperature sites more recently than ~4 AE ago, the crystallization age could be similar to the average ^{39}Ar–^{40}Ar age of 4.39 AE for extractions of 1200°C and above (84% of the ^{39}Ar).

There is only minor evidence in our feldspar sample of ^{40}Ar degassing by a shock-heating event more recently than 4.26 AE ago. If the ^{39}Ar–^{40}Ar profile of Fig. 4 was caused by ^{40}Ar redistribution and represents a K–Ar closure age for the bulk sample of 4.26 AE, then the feldspar has not lost any ^{40}Ar by a more recent heating. Alternatively, the lower ^{39}Ar–^{40}Ar ages shown by the extractions releasing from 1.8% to 16% of the ^{39}Ar

(750°C through 1100°C) are characteristic of a small amount of ^{40}Ar loss from less retentive sites. If the K–Ar closure age is as old as the value of 4.4 AE suggested by the concordant Rb–Sr and Sm–Nd ages of Px 5, then the feldspar could have lost up to ~10% of its ^{40}Ar in a subsequent event. The time of such an event is not uniquely identifiable from the Ar data. However, low apparent ages of ~2.4–3.5 AE occur at comparatively high extraction temperatures of 750°–950°C. These apparent ages are not easily attributed to long-term continuous loss of Ar due, for example, to solar heating, and suggest the occurrence of one or more discrete events which affected the Ar systematics more recently than 3.5 AE ago. This event is probably the same one which affected the Rb–Sr systematics of Px 4 and the sample of dark-brown glass. The devitrification of maskelynite was caused by temperatures in excess of 800°C. Furthermore, the low ages for at least the 850°C and 950°C temperature steps are associated with gas released from maskelynite as shown by the K/Ca ratios. It thus seems probable that the low apparent ages are associated with the shock event and provide an upper bound to the time of occurrence of this event. An alternative possibility is that a major shock event associated with the excavation of the norite boulder occurred quite early and its age is not clearly resolved in our data from the crystallization age. The recent disturbances in the Rb–Sr and K–Ar system must then be attributed to unidentified events, possibly including the one which initiated cosmic ray exposure. We consider this scenario less satisfying and of lower probability than the first.

If a major shock event did occur more recently than 3.5 AE ago, then the observation that the K–Ar systematics of the maskelynite were only affected to a minor extent is further testimony to the Ar retentiveness of 78236 feldspar. We have calculated values of the diffusion parameter, D/a^2 (Fechtig and Kalbitzer, 1966), for ^{39}Ar in 78236,4 feldspar and plotted these in an Arrhenius plot of $\log D/a^2$ vs. reciprocal temperature (Fig. 5). Although all of these data do not give a linear trend consistent with simple diffusion, the data from extractions with constant K/Ca ratios (containing 97% of the ^{39}Ar) do give an approximately linear trend. This trend is nearly parallel to the Arrhenius plots for ^{39}Ar diffusion from plagioclase in lunar rock 14310 (Turner *et al.*, 1973) and from maskelynite in Shergotty (Bogard *et al.*, 1979), but the Arrhenius plot for 78236 is offset downwards from 14310 and Shergotty by 2 to 3 orders of magnitude. The slower diffusion of ^{39}Ar in 78236 feldspar (i.e., lower values of D/a^2) is apparently due to larger values of the diffusion path, a, caused by the coarse grain size of 78236.

Argon diffusion data for 78236 feldspar can be used to estimate some restrictions on the various shock heating models discussed earlier. If 78236 were shock-heated to ~800°C, the minimum required for devitrification of maskelynite, at a time significantly later than the minimum formation age of 4.26 AE, it would have had to cool within days to weeks in order not to have reset the K–Ar age. This implies a very shallow post-shock burial depth of no more than a few meters. Of course, if the shock features were formed at the same time 78236 was excavated from a deep, hot environment which permitted the isotope systems to remain open, the Ar diffusion data would place no real restrictions on post-excavation cooling.

DISCUSSION

From the data presented above, there is little question that the crystallization age of 78236 is ≥ 4.26 AE. Although we favor an age of 4.43 ± 0.05 AE for reasons also given above, there is admittedly some ambiguity in interpretation of the isotopic data. Resolution of this ambiguity is of considerable importance because of the different implications of an "old" age which can be associated with events occurring during early lunar differentiation and of a "young" age which is perhaps more indicative of later local events.

In the following discussion we will address several issues which are related to the choice of a most probable crystallization age. We will first discuss some constraints on the crystallization age which can be derived from various model calculations, and conversely the implications of different crystallization ages to the petrogenesis of the

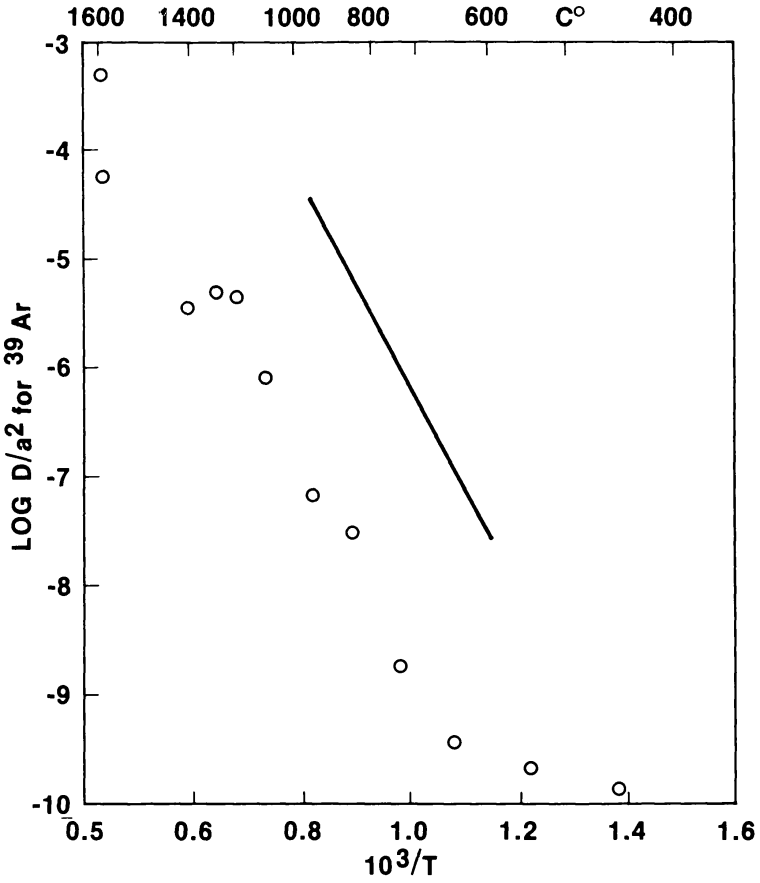

Fig. 5. Arrhenius plot of log D/a^2 versus 1/T ($\times 10^3$) for diffusion of ^{39}Ar from 78236,4 feldspar. The solid line is the analogous trend for feldspar from 14310 (Turner *et al.*, 1973), and is similar to the trend for diffusion of ^{39}Ar from feldspar (maskelynite) from the Shergotty achondrite (Bogard *et al.*, 1979).

norite. We will then discuss whether events related to petrologically observed shock features can be related to any of the observed isotopic disturbances, and if so, to which disturbances. Finally, we will consider the probable effect on the isotopic systems of slow cooling in the lunar crust, remembering that a deep origin has been suggested for 78236 (Jackson *et al.*, 1975).

Implications of model ages and initial isotopic ratios for the age and petrogenesis of 78236

The simplest model ages are those relative to assumed values of the lunar initial $^{87}Sr/^{86}Sr$ and $^{143}Nd/^{144}Nd$. We calculate model ages of 4.48 ± 0.14 AE and 4.63 ± 0.03 AE for initial $^{87}Sr/^{86}Sr = 0.69903$ (LUNI, Nyquist *et al.*, 1973) and initial $^{143}Nd/^{144}Nd = 0.50589$ (Nyquist *et al.*, 1979a), respectively. The comparatively large plagioclase content of 78236 would lead one to expect a significant decrease in Rb/Sr during its formation via plagioclase and orthopyroxene accumulation, and consequently, a Rb–Sr model age which is older than the crystallization age if 78236 is significantly younger than the moon. Similarly, the comparatively large orthopyroxene content of 78236 might be expected to produce a net increase in the Sm/Nd ratio during accumulation and, consequently, a Sm–Nd model age which is younger than the crystallization age. The near-concordance of Rb–Sr and Sm–Nd model ages at values near the lunar formation age argues for an early formation of 78236.

Let us consider the Rb–Sr systematics in more detail. Assume that 78236 has a "young"

crystallization age of, say, 4.27 AE, so that I(Sr) = 0.69912 ∓ 9 as shown by the dotted isochron in Fig. 2. Single stage evolution from LUNI = 0.69903 at 4.56 AE ago would require a time averaged $^{87}Rb/^{86}Sr = 0.022$, i.e., essentially the same as the whole rock value. This comparatively low time averaged value can be compared to estimates of $^{87}Rb/^{86}Sr$ in the parental magma of 78236. Because the plagioclase and orthopyroxene in 78236 are almost totally cumulus, we can estimate Rb/Sr in the parental magma from measured values for mineral separates and the mineral/liquid distribution coefficients. As usual, we use D(Rb, plag) = 0.035 and D(Sr, plag) = 1.5 (Shih *et al.*, 1975). Since

$$\left(\frac{Rb}{Sr}\right)_c = \frac{D(Rb)}{D(Sr)}\left[\frac{Rb}{Sr}\right]_p \quad (1)$$

where subscript "c" denotes "cumulate" and "p" denotes "parental magma", we estimate $(^{87}Rb/^{86}Sr)_p \approx 0.43$ from the plagioclase separate of lowest Rb/Sr ratio (Mask 3). Similarly, using D(Rb, opx) = 0.0091 and D(Sr, opx) = 0.010, we estimate $(^{87}Rb/^{86}Sr)_p \approx 0.44$ from Px 1 which had the lowest Sr content and thus probably was least contaminated with high Sr phases. One can also obtain a similar value of $(^{87}Rb/^{86}Sr)_p = 0.45$ from the whole rock $^{87}Rb/^{86}Sr$ ratio if ~2% of the parental magma is trapped among the accumulating crystals. This amount of trapped liquid is quite reasonable and consistent with the amount of mesostasis measured in 78236 (Table 1). Thus, there are strong arguments that $^{87}Rb/^{86}Sr \approx 0.4$ in the parental magma of 78236 in comparison to the much lower time averaged $^{87}Rb/^{86}Sr = 0.022$ calculated for single stage Sr evolution between 4.56 and 4.27 AE ago. The two results can be reconciled only if the high Rb/Sr magma persisted for only a short time. The most natural explanation is that the high Rb/Sr magma was produced as a residuum of early lunar differentiation prior to 4.43 AE ago and the single stage time averaged value pertains to Sr evolution in the rock itself after its early formation, i.e., the 4.27 AE age is not the crystallization age. We cannot rule out the possibility that a high Rb/Sr magma was produced by partial melting at ~4.27 AE ago from a source with Rb/Sr similar to that of 78236 and that this magma persisted for only a very short time. However, this scenario seems less probable than the previous one because it requires that an increase in Rb/Sr caused by partial melting of the source be nearly exactly compensated by accumulation of 78236. This would require a fortuitous combination of cumulus plagioclase and orthopyroxene plus trapped liquid in just the right proportions to undo the effect of partial melting with respect to the Rb/Sr ratio.

We discuss the Sm–Nd systematics with the aid of the ϵ(Nd)-diagram (Fig. 6). We use the conventional definition

$$\epsilon(Nd, T) = \frac{I(Nd, T, S) - I(Nd, T, R)}{I(Nd, T, R)} \times 10^4$$

where "S" denotes sample, "R" a reference reservoir, and "T" the crystallization age. To maintain internal consistency we use our Sm–Nd data for the eucrites Juvinas and Chervony Kut to calculate I(Nd, T, R) (Nyquist *et al.*, 1979a). These data have been shown by Jacobsen and Wasserburg (1980) to be consistent with the Sm–Nd evolution in chondrites. Using the isochron results for the "most retentive" data, we find $\epsilon(4.43\ AE) = 0.08 \pm 0.4$ which is our preferred value for this parameter. The isochron results, including data from all mineral separates, gives $\epsilon(4.33\ AE) = 0.8 \pm 0.9$. The error limits are calculated without including the error of the reference value, but the errors of both the reference and analytical data are shown in Fig. 6. The latter value is in good agreement with $\epsilon(4.34\ AE) = 1.1$ previously reported by Carlson and Lugmair (1981). These positive ϵ-values obtained from isochron data are qualitatively consistent with a model age > 4.56 AE for the whole rock analysis.

It is unclear at this stage how much significance should be attached to these positive ϵ-values because the analytical uncertainties are such that they could be consistent with "chondritic" evolution at the extreme error limits. Analyses of three norite clasts and a

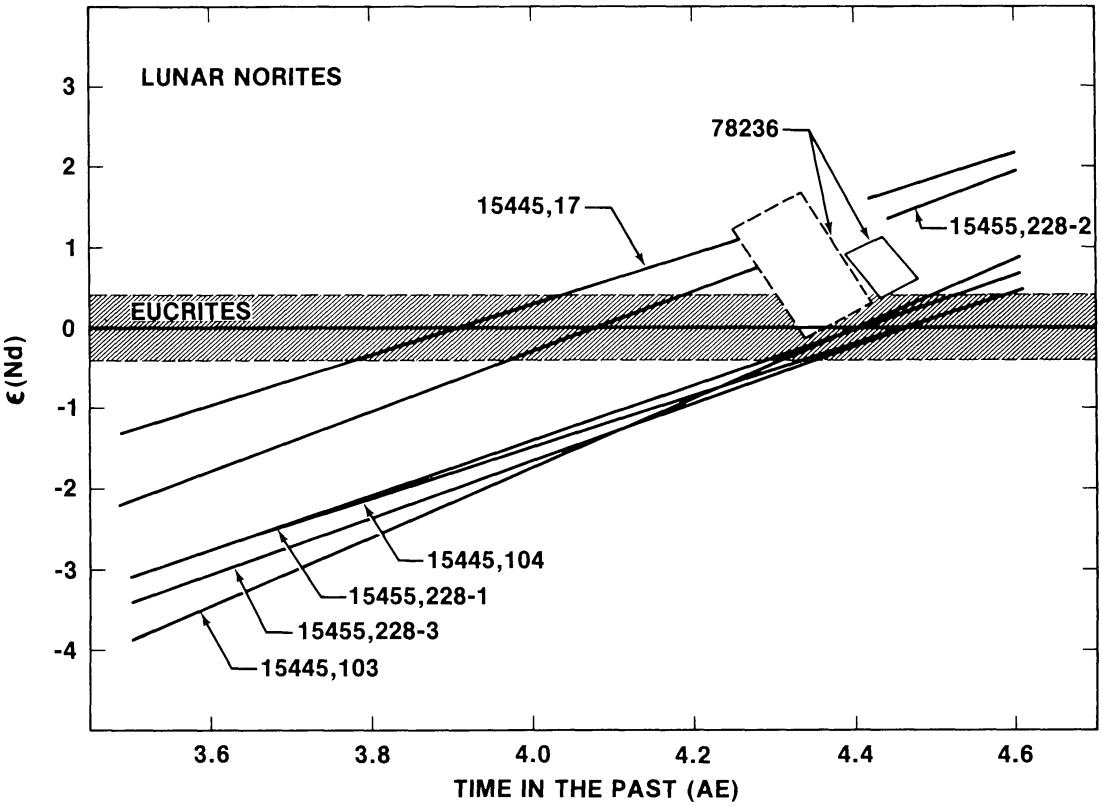

Fig. 6. Deviation of $^{143}Nd/^{144}Nd$ from "chondritic" evolution in parts in 10^4 for 78236, other lunar norite clasts from 15445 and 15455 and spinel troctolite 15445,103 (lithology 45C of the Imbrium Consortium, see Ryder and Bower, 1977). Data for Apollo 15 clasts are unpublished analyses done at JSC. Error limits are typically $\pm 0.6\epsilon$-unit where not shown. Solid box shows our preferred parameters for 78236; dotted box includes all our Sm–Nd data and is comparable to T = 4.34 AE, $\epsilon(Nd) = 1.1$ reported by Carlson and Lugmair (1980). In general $\epsilon(Nd, 4.2\ AE) \sim 0$, whereas $\epsilon(Nd, 4.4\ AE) \gtrsim 0$.

spinel troctolite clast from 15455 and 15445 give $\epsilon \sim 0$ at ~ 4.4 AE (Fig. 6). However, two analyses of norite clasts from 15445 and 15455 give higher ϵ-values, somewhat greater than that of 78236. Carlson and Lugmair (1980) report $\epsilon(4.23\ AE) = 0.5 \pm 1.4$ for 73255,27,45. This value plots on the line shown for 15455,228-2 in Fig. 6, with error limits overlapping the "chondritic" evolution line. Continuing work is needed to show whether or not $\epsilon(4.4\ AE) > 0$ for lunar norites.

Positive ϵ-values at 4.4 AE could be interpreted as favoring young crystallization ages in the vicinity of 4.2 AE where $\epsilon \sim 0$. However, this interpretation entails the *assumption* that the time averaged Sm/Nd ratio prior to formation of the rock should be "chondritic". It is not clear that this should be the case since the precursor material should have been influenced by prior global lunar differentiation. One can calculate the Sm/Nd ratio in the parental magma of 78236 by an equation analogous to Eq. (1). As for our mare basalt modeling (cf. Nyquist *et al.*, 1979a), we use D(Nd, opx) = 0.014 and D(Sm, opx) = 0.022 from Weill and McKay (1975). Assuming $^{147}Sm/^{144}Nd = 0.397$ from Px-4 of Carlson and Lugmair (1981), we estimate $(^{147}Sm/^{144}Nd)_p = 0.25$ for the parental magma. Similarly, using the distribution coefficients given by Shih *et al.* (1975), we estimate $(^{147}Sm/^{144}Nd)_p = 0.18$ from $^{147}Sm/^{144}Nd = 0.14$ for plagioclase separates with the lowest Sm/Nd ratios. The agreement between these values is not very good, but can be attributed to uncertainties in the distribution coefficients and to the fact that the Sm/Nd ratios of the minerals are severely fractionated from that of the parental magma. A more reliable estimate of $(Sm/Nd)_p$ could be made from the Sm/Nd ratio of the whole rock if the amount of trapped liquid were known. Consistency with the above calculations of $(Rb/Sr)_p$ and the

total modal abundance of mesostasis requires about 2% trapped liquid. In this case we calculate $\bar{D}(Sm)/\bar{D}(Nd) = 1.01$ and $(^{147}Sm/^{144}Nd)_p = 0.170$ from the whole rock value of $^{147}Sm/^{144}Nd = 0.1724$. It is noteworthy that this corresponds to $^{147}Sm/^{144}Nd = 0.175$ at 4.4 AE ago as we have used for our mare basalt models (Nyquist *et al.*, 1979a). However, such a low Sm/Nd ratio is not consistent with a simple single stage model of Nd isotopic evolution from chondritic initial values to $\epsilon(4.2\text{–}4.4) \geq 0$ for 78236. Perhaps this result is not surprising in view of the paradoxical evidence that trace element abundances of 78236 imply an evolved trace element rich parental magma (Blanchard and McKay, 1981; Carlson and Lugmair, 1981), whereas the high atomic Mg/Mg + Fe value implies a "primitive" parental magma. Longhi (1980) has described complex petrogenetic processes which might take place in a lunar magma ocean to give rise to the non-chondritic Ca/Al ratios and REE abundances required of the parental magmas of pristine plutonic lunar rocks. A decoupling of $^{147}Sm/^{144}Nd$ and $^{143}Nd/^{144}Nd$ ratios during these complex crystallization and assimilative processes is not unexpected. The basic cause of $^{143}Nd/^{144}Nd$ in the magma greater than that supported by simple radiogenic growth is the operation of fractionation processes which act to decrease the Sm/Nd ratio relative to the time-averaged value. Decreased Sm/Nd implies a general LREE enrichment which was one of the features which Longhi's model was constructed to reproduce. A value of $^{143}Nd/^{144}Nd$ in the magma which is greater than that in a chondritic reservoir of the same age ($\epsilon > 0$) implies the additional constraint that Nd is being supplied to the magma from reservoirs having $^{147}Sm/^{144}Nd$ greater than chondritic. Such reservoirs could be earlier-formed pyroxene cumulates which upon being partially remelted and reassimilated give rise to magmas with lower Sm/Nd but the same $^{143}Nd/^{144}Nd$ as the parental cumulates. When these partial melts mix back into the main magma ocean, they would make $\epsilon > 0$ in the resultant mixed magma.

The role of shock metamorphism

During the last decade, a large number of Rb–Sr and K–Ar isotopic studies on shock-metamorphosed samples have been carried out. Wolfe (1971) and Hartung *et al.* (1971) have shown that the K-Ar system of shock-metamorphic feldspar clasts in terrestrial impact melts could be completely reset, but that an extensive *thermal* annealing is necessary to achieve complete degassing of radiogenic argon. Many shock metamorphosed breccias, even those shocked to pressures up to 50 GPa, were shown to be incompletely outgassed. For a series of lithic clasts derived from the suevite of the Noerdlinger Ries, Bogard *et al.* (1981) found ^{39}Ar–^{40}Ar ages consistent with the time of impact (~15 m.y.). On the other hand, Jessberger *et al.* (1978) analyzed several samples shocked to very similar degrees as those analyzed by Bogard *et al.* (1981) but from the fractured basement of the Ries Crater (ages ~300 m.y.) and could not detect any resetting of the K–Ar clock in these samples. We think that the samples analyzed by Jessberger *et al.* (1978) were less thermally annealed than the clasts from the suevite.

It has been shown that it is easier to reset the Rb–Sr system of severely shocked samples than of less shocked ones, but this was only observed in *thermally* metamorphosed feldspar clasts of increasing shock metamorphism from the Lappajaervi impact melt (Reimold, 1980). Thus, it is doubtful that *shock alone* has a significant influence on the isotopic systematics of shock metamorphic samples. We prefer to interpret the observed isotopic disturbances as due to post-shock *thermal* metamorphism of the norite, as could be achieved by the incorporation of the shocked sample into a hot impact breccia or ejecta blanket.

In the petrography section of this paper, two models were outlined for a probable shock and thermal history of 78236. For petrographic and chemical reasons a one-stage impact history of the norite is preferred. The isotopic results lend further support to the one-stage model. A second impact that caused part of the rock to melt should be identifiable in the isotopic results, especially in the ^{39}Ar–^{40}Ar study. Also, the Rb–Sr isochron age defined by the four most reset samples—including a separate of norite

melt—clearly gives evidence for a single strong event that re-equilibrated part of the rock. The slight Ar isotopic disturbances produced $\lesssim 3.5$ AE ago in the norite are probably related to a thermal event that caused the maskelynite to recrystallize at temperatures above 800°C. We suggest that a single "recent" event affected the Rb–Sr and K–Ar systems no earlier than 3.5 AE ago.

Slow cooling of 78236 in the lunar crust?

In spite of clear evidence of extensive shock metamorphism accompanied by disturbances of the isotopic systems, there is reason to believe that not all of these disturbances can be attributed to shock. The ^{39}Ar–^{40}Ar data provide perhaps the most direct support for this belief. 94% of the ^{39}Ar in the maskelynite is very retentively sited and is released only above 1100°C, and 84% of the ^{39}Ar is released only above 1200°C. It is difficult to see how comparatively moderate post-shock temperatures could have affected the $^{40}Ar/K$ ratio of these retentive sites. Furthermore, the K/Ca ratio at these high temperatures is extremely constant, indicating that the Ar released is coming from a single phase, plagioclase. It is thus difficult to account for variations in apparent age of the high temperature gas release as due to redistribution of Ar among different phases by the recent shock event.

Less direct but analogous arguments can be made for the other isotopic systems. The scatter of the Sm–Nd data is particularly difficult to understand. Fractionation of the Sm/Nd ratio is very difficult and REE diffusion is very sluggish (Magaritz and Hofmann, 1978b). Furthermore, cation diffusion rates in pyroxene are very slow compared to other minerals which have been studied (see Nyquist *et al.*, 1979b, for a summary). Finally, pyroxene and plagioclase grains in 78236 can be several mm in size, further increasing the difficulty of isotopic exchange. These considerations, which will be quantified below, make it extremely difficult to accept post-shock thermal annealing as the cause of isotopic disturbances in the Sm–Nd system of 78236.

The need for a non-shock related cause is less apparent for the Rb–Sr system. At least the most aberrant data must be related to post-shock thermal annealing. However, as discussed above, the observed disturbances are most reasonably attributed to small amounts of contaminating phases such as mesostasis in some of the pyroxene separates. Pyroxene itself should be very resistant to diffusion of Sr necessary for isotopic exchange. The data of Sneeringer and Hart (1978) for Sr diffusion in diopside can be represented by the Arrhenius equation

$$D(\mathrm{Sr, px}) = 1.8 \times 10^{7} \exp\left[-\frac{66{,}500}{T}\right] \mathrm{cm^2\ sec^{-1}} \tag{2}$$

where "T" is absolute temperature and "D" is the diffusion rate. For the approximation of spherical grains of radius $a = 1$ mm one has

$$\frac{D}{a^2}(\mathrm{Sr, px}) = 1.8 \times 10^{9} \exp\left[-\frac{66{,}500}{T}\right] \mathrm{sec^{-1}}. \tag{3}$$

For T = 850°C we find $D/a^2 = 3.5 \times 10^{-17}$ sec^{-1}. In contrast, Sr diffusion in obsidian glass may be characterized by (Brown *et al.*, 1975)

$$D(\mathrm{Sr, obs}) = 0.09 \exp\left[-\frac{21{,}900}{T}\right] \mathrm{cm^2\ sec^{-1}}. \tag{4}$$

The latter may be appropriate for Sr diffusion in mesostasis of effective radius $a \sim 100\ \mu$m so that

$$\frac{D}{a^2}(\mathrm{Sr, mes}) = 9 \times 10^{2} \exp\left[-\frac{21{,}900}{T}\right] \mathrm{sec^{-1}}. \tag{5}$$

In this case we have $D/a^2 = 3 \times 10^{-6}$ sec^{-1} for T = 850°C. Using $Dt/a^2 \sim 1$ as an estimate of the time required for complete isotopic exchange, one sees that isotopic exchange in mesostasis could be achieved within a few days. For pyroxene, however, Dt/a^2 would have reached only $\sim 10^{-11}$ so that Sr migration would be trivial. In fact, any significant migration of Sr in pyroxene at this temperature would seem to require millions of years and an ejecta blanket thickness of tens of kilometers (see Fig. 5 in Nyquist *et al.*, 1979b). Given this great disparity in susceptibility to isotopic exchange among phases which contribute to the Sr inventory of our pyroxene separates, observation of isotopic disturbances becomes easily understandable. However, we must infer that any mesostasis in separate Px 5 must be effectively armoured by surrounding pyroxene in order for the 4.38 AE age to have been preserved. Such an armoring effect has been previously suggested by Papanastassiou and Wasserburg (1975) for olivine separates of lunar troctolite 76535. Furthermore, there is no evidence of mesostasis contamination of Px 2; this separate in fact has a high Sm/Nd ratio which is totally consistent with pure orthopyroxene. One is thus left without an effective explanation of the 0.28 ± 0.09 AE difference in pyroxene-whole rock ages of these two samples.

The explanation which we offer for these observations is that 78236 probably cooled very slowly after its crystallization. Slow cooling is expected from the large grain size and the suggested deep origin (8–30 km, Jackson *et al.*, 1975) of 78236. During this slow cooling, we envision that some minerals closed to isotopic exchange early because of large grain size and/or low diffusion rates. Other minerals closed much later because of small grain size and/or high diffusion rates.

We consider the probable effects on the Sr and Nd isotopic systems of cooling from the solidus temperature of ~1100°C at a depth of 50 km in the moon according to the model of Toksöz *et al.* (1978). Although several lunar thermal models have been presented in the literature, their differences are not important for our discussions. The depth chosen is admittedly a more extreme situation than the 8–30 km depth previously suggested (Jackson *et al.*, 1975) and it is chosen partly for convenience in use of the thermal model calculations. A deep origin presumes that 78236 crystallized near the base of the lunar crust. The cooling rate at this depth is relatively slow; the temperature changes by only 20% in the first 600 m.y. as indicated by the dotted line and right-hand scale in Fig. 7. We have calculated values of D/a^2 at intervals from the onset of cooling according to Eq. (3) for Sr diffusion in pyroxene. These values of D/a^2 multiplied by t, the time since the beginning of cooling, are shown on curve A in Fig. 7. We interpret this and analogous curves as follows.

At very early times temperature, T, and D/a^2 are very nearly constant. Dt/a^2 increases approximately linearly with time t and soon exceeds the "threshold" value $Dt/a^2 = 1$. The system is now considered to be open since any radiogenic Sr initially present in a grain would have sufficient time to diffuse out of that grain. [See Nyquist *et al.* (1979b) for further explanation of this criterion.] We thus define $t_0 = a^2/D(T_0)$ as the time of system opening. There is a period of time subsequent to t_0 when $Dt/a^2 \gg 1$. The system is open throughout this interval. Although D/a^2 is continually decreasing, it is still sufficiently large so that only a small portion Δt of the total elapsed time is required for $D\Delta t/a^2 = 1$ so that a radiogenic atom produced near the center of the grain can migrate out in time Δt. During this open system interval radiogenic atoms migrate out of the grain nearly as fast as they are produced. They are replaced by other Sr atoms which are presumed present at the surface of the grain so that isotopic equilibration is achieved between the exterior and interior Sr. However, when D/a^2 has fallen such that $Dt/a^2 \approx 1$ again, the time necessary for a radiogenic Sr atom to diffuse out is comparable to the total elapsed time and the system may be considered closed. This can be intuitively seen by considering a radiogenic Sr atom produced near the center of the grain at the closure time t_c defined by $t_c = a^2/D(T_c)$ where T_c is the corresponding closure temperature. Such an atom would require a time comparable to t_c to migrate from the grain. However, within a short time, Δt, D/a^2 has fallen drastically and the migration time extended proportionately. If $D(t_c + \Delta t)/a^2$ is considered, the time required for atomic migration from the grain is

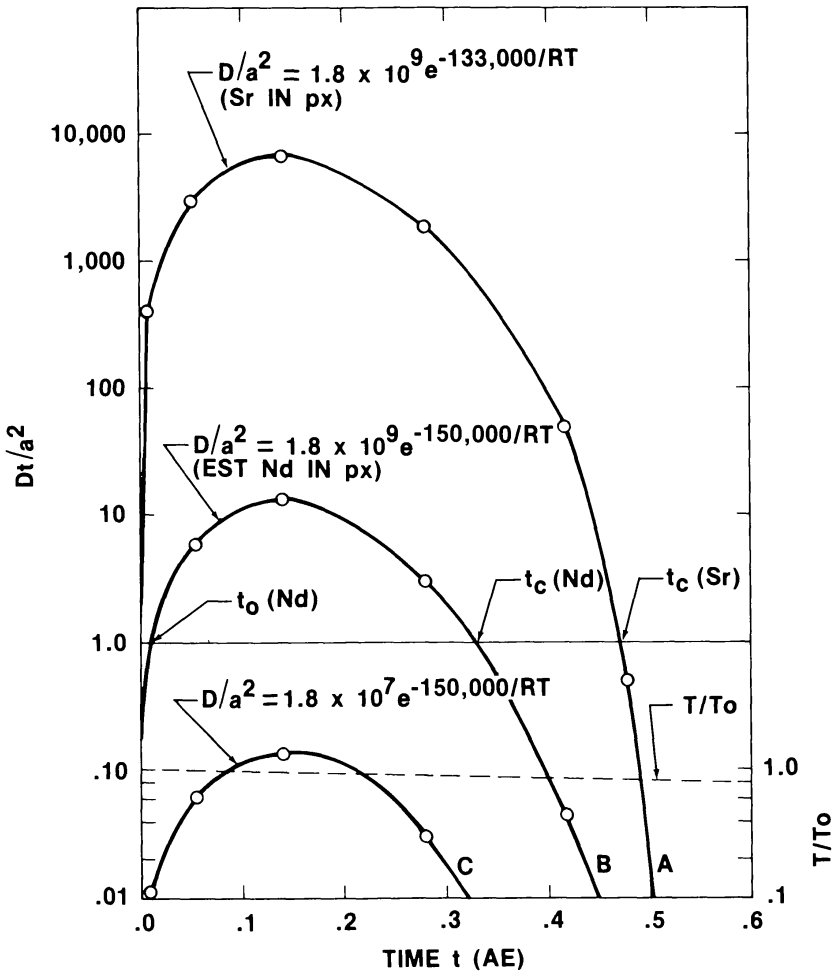

Fig. 7. Temperature T/T_0 (dashed curve) and diffusion parameter Dt/a^2 as a function of time t for a depth of 50 km in the lunar crust. T/T_0 is interpolated from the lunar thermal model given in Fig. 8 of Toksöz *et al.* (1978) for $T_0 = 1100°C$. The Arrhenius relation for curve A is derived from the data of Sneeringer and Hart (1978) for $a = 1$ mm. The Arrhenius relation for curve B was estimated by assuming the same pre-exponential factor as for curve A, but a 17 kcal/mole higher activation energy (see text). Curve C is the same with $a = 1$ cm. Because characteristic times in thermal models scale inversely with the square of depth, the curves will shrink towards the origin for shallower depths. Effective times of system opening (t_0) and closing (t_c) correspond to points where the curves cross $Dt/a^2 = 1$.

several times greater than $(t_c + \Delta t)$, and so on. Thus, atomic migration from the grain effectively ceases within a short time after t_c and the system may be considered closed. For the example illustrated here, the open system interval $t_c - t_0 \approx 0.5$ AE.

Let us now consider the case for Nd diffusion. To the best of our knowledge, there is currently no available data on Nd diffusion in pyroxene. However, the activation energy for Eu^{3+} diffusion in obsidian is ~15 kcal/mole greater than that of Sr (Magaritz and Hofmann, 1978a,b) whereas the pre-exponential factors are similar. We thus estimate an Arrhenius relation for Nd in pyroxene by assuming the same pre-exponential factor as for Sr in pyroxene and an activation energy of 150 kcal/mole. That is, we estimate

$$\frac{D}{a^2}(\mathrm{Nd, px}) = 1.8 \times 10^9 \exp\left[-\frac{75{,}000}{T}\right] \mathrm{cm^2\ sec^{-1}} \qquad (6)$$

where we have used the fact that the gas constant $R \approx 2$ kcal/mole and again assume $a = 1$ mm.

The values of Dt/a^2 estimated for Nd in pyroxene are shown as curve B in Fig. 7. This curve rises to a lower maximum than does the Sr curve and suggests a closure time which occurs about 0.15 AE sooner than the Sr closure. Curve C illustrates a Nd system for which $a = 1$ cm. This system is effectively always closed to Nd diffusion because Dt/a^2 is always $\lesssim 0.1$.

The foregoing discussion illustrates that even the most resistant radiometric systems of plutonic rocks crystallizing in the hypothetical environment considered will probably remain open for significant but variable times. Unfortunately, the present evidence as to whether 78236 actually conformed to this scenario is non-definitive. On the one hand, the scenario of slow crustal cooling seems a natural way to produce minor isotopic disturbances or discordances. On the other hand, there are details of the 78236 data which seem to require additional explanation. Specifically, the various isotopic systems seem to show more similarities than expected from the crustal cooling model. Thus, if the parameters used in constructing Fig. 7 are approximately correct, it would seem that even partial resetting of the Sm–Nd systematics would imply total resetting of the Rb–Sr systematics. In particular, it is difficult to account for the concordance of the Px 5 separate in the Rb–Sr and Sm–Nd systems if Sr and Nd diffusion rates are as different as we have assumed here. In fact, existing data for Al, Sr, Ca, and U diffusion in pyroxene at 1200°–1300°C indicate similar diffusion rates for these elements. We must await future experimental work to see whether Sr and Nd diffusion rates in pyroxene are significantly different, as we have assumed in constructing Fig. 7, or more similar, as seems most consistent with the slow cooling model.

Explaining the ^{39}Ar–^{40}Ar data in the context of the slow cooling model also requires some further consideration. In this case, we know the diffusion properties of Ar in maskelynite as determined in the stepwise Ar extraction (Fig. 5). As previously discussed, D/a^2 values are two to three orders of magnitude lower than for 14310 (Turner *et al.*, 1973). Nevertheless, D/a^2 in the temperature range of 900°–1100°C is still several orders of magnitude higher than the D/a^2 values which we have used in constructing Fig. 7 for Sr and Nd diffusion in pyroxene. A curve analogous to curve A of Fig. 7 constructed with the Ar diffusion parameters would show a closure time t_c occurring ~2 AE after the onset of cooling. The physical grain size of maskelynite in the rock is, of course, greater than in the analyzed sample. However, decreasing D/a^2 a hundredfold only decreases t_c to ~1.5 AE. It is clear that Ar can rapidly diffuse out of the grains in which it is produced during the entire cooling interval of 1100°–900°C that we have considered for Sr and Nd diffusion. To make $Dt/a^2 \sim 1$ for Ar in maskelynite some 600 m.y. after cooling begins would require an effective a of ~10 meters.

These considerations raise a fundamental question about K–Ar systematics of deeply buried crustal rocks. If Ar can be considered lost as soon as it migrates from the grain in which it is produced, then the only way to start the Ar-clock is to excavate the rock to the surface where it can cool and start retaining Ar. If, however, the maskelynite grains themselves are contained within a larger closed mega-system, the Ar will simply migrate from grain to grain. In the former case we would conclude that if 78236 were formed at considerable depth, then it must have been excavated to the lunar surface prior to 4.2 AE ago and possibly as early as 4.4 AE ago. Alternatively, in the second case the excavation event would not be clearly recorded in the Ar-systematics. However, one would expect to see some age anomalies, because a portion of the Ar currently within a given grain would not have been produced in that grain. In the special case of a monomineralic rock, the anomalies could be negligibly small because all grains would maintain the same steady state ratio of radiogenic Ar to parent K. In the case of 78236, much of the K is in plagioclase as seen from a comparison of whole rock $K_2O \sim 0.04\%$ (Blanchard, pers. comm.) to K_2O in plagioclase of ~0.1% (Table 4). Thus, in the closed mega-system scenario one expects to see approximately uniform ages with some anomalies. This is in fact observed. It seems possible to reconcile the Ar data with the deep origin, slow cooling model in this manner.

If one adopts the closed mega-system argument for the Ar data, it is very difficult to

define an excavation age for 78236. There is some evidence in all three radiometric systems for ages of ~4.2 AE (see also Carlson and Lugmair, 1981). Excavation would truncate the Dt/a^2 curves of Fig. 7 at a common time for all systems. The indications of ~4.2 AE ages might reflect such a truncation, but this identification cannot be strongly defended.

SUMMARY AND CONCLUSIONS

We propose the following chronology for 78236 as the one which seems most consistent with radiometric and other evidence:

1. Cumulate norite 78236 formed deep in the lunar crust ~4.4 AE ago as indicated by concordant Rb–Sr and Sm–Nd ages of the Px 5 separate and by the average age of the last ~60% of the ^{39}Ar–^{40}Ar age spectrum.
2. It cooled slowly in the crust until it was excavated by a major basin-forming event. Excavation may have occurred about 4.2 AE ago, but the time of this event is not well constrained.
3. A secondary event occurred $\lesssim$3.5 AE ago (Rb–Sr isochron of most reset samples and lowest apparent ages of ^{39}Ar–^{40}Ar spectrum). The shock and thermal annealing which produced shock melt, maskelynization of feldspar, and subsequently the devitrification of maskelynite is most reasonably identified with this event. Since there is no independent evidence for basin-forming events as late as 3.5 AE ago, we infer that the shock features were produced during cratering of pre-existing basin ejecta. It seems unlikely that the shock features were produced in the same event which caused onset of exposure to cosmic rays ~290 m.y. ago. If so, it is fortuitous that partial Sr-isotopic exchange occurred for the "most reset" samples in such a manner that they are now aligned on the same ~3.5 AE isochron within error limits. The petrographic observations given earlier in the paper also suggest that the shock and cosmic ray exposure events were distinct.

Alternate explanations of the isotopic data are possible but seem to us to leave more paradoxes than the scenario suggested above. For example, a shallow, late (~4.2–4.3 AE) origin might be suggested. All isotopic disturbances would then be uncritically ascribed to the recent shock event. A major paradox would be: Why was the ^{39}Ar–^{40}Ar age relatively little affected by the shock event, whereas the other ages, particularly the Sm–Nd age, were significantly disturbed? Further study of the chronology of 78236 appears justified. Of special usefulness would be a search for fissiogenic Xe from ^{244}Pu decay, and ^{39}Ar–^{40}Ar and Rb–Sr analyses of the glass covering a part of the boulder.

Finally, it is emphasized that radiometric ages of lunar plutonic rocks of possible deep crustal origin cannot be uncritically accepted as crystallization ages. Temperatures at depth in the crust may well have been high enough to maintain most, or even all, radiometric systems open for a significant period after crystallization. For the Rb–Sr and Sm–Nd systems the closure times could be critically dependent on the mineral grain size. This would appear to be an area of particular concern in the dating of small clasts from breccias as these clasts must be comparatively fine grained in order to have retained an identity as lithic rather than mineral fragments.

Acknowledgments—We would like to acknowledge gratefully the improvement of this paper by fruitful discussions with Doug Blanchard and Gordon McKay. One of us (W.U. Reimold) wishes to express his thanks to the German Science Foundation (Deutsche Forschungsgemeinschaft) for financial support during his stay at the NASA Johnson Space Center, Houston, and the Lunar and Planetary Institute, Houston. We thank Pratt Johnson for support in the Ar analyses. Insightful reviews by G. Lugmair and D. Papanastassiou improved the clarity of presentation of the paper.

The second author (W. Reimold) is a Visiting Scientist at the Lunar and Planetary Institute. The Lunar and Planetary Institute is operated by the Universities Space Research Association under Contract No. NASW-3389 with the National Aeronautics and Space Administration. This paper constitutes the Lunar and Planetary Institute Contribution No. C-455.

REFERENCES

Arndt J. and Gonzalez-Cabeza I. (1981) Diaplectic glass and fusion-formed glass: Comparative studies on shocked anorthosite from Manicouagan Crater, Canada (abstract). In *Lunar and Planetary Science XII*, p. 28–30. Lunar and Planetary Institute, Houston.

Blanchard D. P. and McKay G. A. (1981) Remnants from the ancient lunar crust III: Norite 78236 (abstract). In *Lunar and Planetary Science XII*, p. 83–85. Lunar and Planetary Institute, Houston.

Bogard D. D., Husain L., and Wright R. J. (1976) ^{40}Ar–^{39}Ar dating of collisional events in chondrite parent bodies. *J. Geophys. Res.* **81**, 5664–5678.

Bogard D. D., Husain L., and Nyquist L. E. (1979) ^{40}Ar–^{39}Ar age of the Shergotty achondrite: Implications for its post-shock thermal history. *Geochim. Cosmochim. Acta* **43**, 1047–1055.

Bogard D. D., Hörz F., Johnson P., and Stöffler D. (1981) Resetting of ^{40}Ar–^{39}Ar ages in suevite ejecta from the Ries Crater (abstract). In *Lunar and Planetary Science XII*, p. 92–95. Lunar and Planetary Institute, Houston.

Brown L., Hofmann A. W., Magaritz M., and Pepper G. H. (1975) Diffusion in silicate melts and glasses. *Carnegie Inst. Wash., Yearb.* **75**, p. 249–259.

Carlson R. W. and Lugmair G. W. (1980) 78236, a primary, but partially senile lunar norite (abstract). In *Lunar and Planetary Science XI*, p. 125–127. Lunar and Planetary Institute, Houston.

Carlson R. W. and Lugmair G. W. (1981) Time and duration of lunar highland crust formation. *Earth Planet. Sci. Lett.* **52**, 227–238.

Curtis D. B. and Wasserburg G. J. (1975) Apollo 17 neutron stratigraphy-sedimentation and mixing in the lunar regolith. *The Moon* **13**, 185–227.

Drozd R. J., Hohenberg C. M., Morgan C. J., Podosek F. A., and Wroge M. L. (1977) Cosmic-ray exposure history at Taurus-Littrow. *Proc. Lunar Sci. Conf. 8th*, p. 3027–3043.

Duke M. B. (1968) The Shergotty meteorite: Magmatic and shock metamorphism features. In *Shock Metamorphism of Natural Materials* (B. M. French and N. M. Short, eds.), p. 613–621. Mono, Baltimore.

El Goresy A., Engelhardt W. v., Arndt J., and Mangliers D. (1976) Shocked norite 78235: Primary textures and shock features (abstract). In *Lunar Science VII*, p. 239–241. The Lunar Science Institute, Houston.

Fechtig H. and Kalbitzer S. (1966) The diffusion of argon in potassium-bearing solids. In *Potassium–Argon Dating* (O. A. Schaeffer and J. Zahringer, eds.), p. 68–107. Springer-Verlag, N.Y.

Gast P. W., Hubbard N. J., and Wiesmann H. (1970) Chemical composition and petrogenesis of basalts from tranquility base. *Proc. Apollo 11 Lunar Sci. Conf.*, p. 1143–1163.

Gibbons R. V. and Ahrens T. J. (1974) Experimental shock metamorphism of labradorite and bronzite (abstract). *Abstracts with Program, Geol. Soc. Amer.* **6**, p. 752.

Hart S. R. (1964) The petrology and isotopic-mineral age relations of a contact zone in the Front Range, Colorado. *J. Geol.* **72**, 493–525.

Hartung J. B., Dence M. R., and Adams J. A. (1971) Potassium-argon dating of shock-metamorphosed rocks from the Brent impact crater, Ontario, Canada. *J. Geophys. Res.* **76**, 5437–5448.

Hofmann A. W. and Margaritz M. (1975) Diffusion in silicate melts and glasses. *Carnegie Inst. Wash., Yearb.* **75**, p. 249–259.

Hofmann A. W. and Magaritz M. (1977) Diffusion of Ca, Sr, Ba, and Co in basalt melt: Implications for the geochemistry of the mantle. *J. Geophys. Res.* **82**, 5432–5540.

Jackson E. D., Sutton R. L., and Wilshire H. G. (1975) Structure and petrology of a cumulus norite boulder sampled by Apollo 17 in Taurus-Littrow Valley, the Moon. *Geol. Soc. Amer. Bull.* **86**, 433–442.

Jacobsen S. B. and Wasserburg G. J. (1980) Sm–Nd isotopic evolution of chondrites. *Earth Planet. Sci. Lett.* **50**, 139–155.

Jessberger E. K., Staudacher T., Dominik B., Kirsten T., and Schaeffer O. (1978) Limited response of the K–Ar system to the Nördlinger Ries giant meteorite impact. *Nature* **271**, 338–339.

Lingenfelter R. E., Canfield E. H., and Hampel V. E. (1972) The lunar neutron flux revisited. *Earth Planet. Sci. Lett.* **16**, 355–369.

Longhi J. (1980) A model of early lunar differentiation. *Proc. Lunar Planet. Sci. Conf. 11th*, p. 289–315.

Lugmair G. W. and Scheinin N. B. (1975) Sm–Nd systematics of the Stannern meteorite (abstract). *Meteoritics* **10**, 447–448.

Lugmair G. W., Scheinin N. B., and Marti K. (1975) Sm–Nd age and history of Apollo 17 basalt 75075: Evidence for early differentiation of the lunar exterior. *Proc. Lunar Sci. Conf. 6th*, p. 1419–1429.

Lugmair G. W. and Marti K. (1977) Sm–Nd–Pu timepieces in the Angra Dos Reis meteorite. *Earth Planet. Sci. Lett.* **35**, 273–284.

Lugmair G. W. and Carlson R. W. (1979) Sm–Nd constraints on early lunar differentiation and the evolution of KREEP. *Earth Planet. Sci. Lett.* **45**, 123–132.

Magaritz M. and Hofmann A. W. (1978a) Diffusion of Sr, Ba, and Na in obsidian. *Geochim. Cosmochim. Acta* **42**, 595–605.

Magaritz M. and Hofmann A. W. (1978b) Diffusion of Eu and Gd in basalt and obsidian. *Geochim. Cosmochim. Acta* **42**, 847–858.
McCallum I. S. and Mathez E. A. (1975) Petrology of noritic cumulates and a partial melting model for the genesis of Fra Mauro basalts. *Proc. Lunar Sci. Conf. 6th*, p. 395–414.
McCallum I. S., Mathez E. A., Okamura F. P., and Ghose S. (1975) Petrology of noritic cumulates: Samples 78235 and 78238 (abstract). In *Lunar Science VI*, p. 534–536. The Lunar Science Institute, Houston.
Mehta S. and Goldstein J. I. (1980) Metallic particles in the glass coatings of lunar highland samples 65315, 67435, and 78235 (abstract). In *Lunar and Planetary Science XI*, p. 720–722. Lunar and Planetary Institute, Houston.
Nyquist L. E., Hubbard N. J., Gast P. W., Bansal B. M., Wiesmann H., and Jahn B. (1973) Rb–Sr systematics for chemically defined Apollo 15 and 16 materials. *Proc. Lunar Sci. Conf. 4th*, p. 1823–1846.
Nyquist L. E., Shih C.-Y., Wooden J. L., Bansal B. M., and Wiesmann H. (1979a) The Sr and Nd isotopic record of Apollo 12 basalts: Implications for lunar geochemical evolution. *Proc. Lunar Planet. Sci. Conf. 10th*, p. 77–114.
Nyquist L. E., Wooden J., Bansal B., Wiesmann H., McKay G., and Bogard D. D. (1979b) Rb–Sr age of the Shergotty achondrite and implications for metamorphic resetting of isochron ages. *Geochim. Cosmochim. Acta* **43**, 1057–1074.
Nyquist L. E., Reimold W. U., Wooden J. L., Bansal B. M., Wiesmann H., and Shih C.-Y. (1981) Sr and Nd cooling ages of cumulate norite 78236 (abstract). In *Lunar and Planetary Science XII*, p. 782–784. Lunar and Planetary Institute, Houston.
Papanastassiou D. A. and Wasserburg G. J. (1976) Rb–Sr age of troctolite 76535. *Proc. Lunar Sci. Conf. 7th*, p. 2035–2054.
Reimold W. U. (1980) Isotopen-, Haupt- und Spurenelement-Geochemie und Petrographie der Impaktschmelzen des Lappajärvi-Kraters, Finnland. Ph.D. Thesis, Westf. Wilh. Univ., Münster, FRG.
Reimold W. U. and Stöffler D. (1978) Experimental shock metamorphism of dunite. *Proc. Lunar Planet. Sci. Conf. 9th*, p. 2805–2824.
Russ G. P., Burnett D. S., Lingenfelter R. E., and Wasserburg G. J. (1971) Neutron capture on ^{149}Sm in lunar samples. *Earth Planet. Sci. Lett.* **13**, 53–60.
Ryder G. and Bower J. F. (1977) Petrology of Apollo 15 black-and-white rocks 15445 and 15455—Fragments of the Imbrium impact melt sheet? *Proc. Lunar Sci. Conf. 8th*, p. 1895–1923.
Schaal R. B., Hörz F., Thompson T. D., and Bauer J. F. (1979) Shock metamorphism of granulated lunar basalt. *Proc. Lunar Planet. Sci. Conf. 10th*, p. 2547–2571.
Sclar C. B. and Bauer J. F. (1975) Shock-induced subsolidus reduction-decomposition of orthopyroxene and shock-induced melting in norite 78235 (abstract). In *Lunar Science VI*, p. 730–732. The Lunar Science Institute, Houston.
Sclar C. B. and Bauer J. F. (1976) Subsolidus reduction phenomena in lunar norite 78235: Observations and interpretations. *Proc. Lunar Sci. Conf. 7th*, p. 2493–2508.
Shih C.-Y., Haskin L. A., Wiesmann H., Bansal B. M., and Brannon J. C. (1975) On the origin of high-Ti mare basalts. *Proc. Lunar Sci. Conf. 6th*, p. 1255–1285.
Shih C.-Y., Nyquist L. E., Bansal B. M., Wiesmann H., Wooden J. L., and McKay G. A. (1981) REE, Sr, and Nd isotopic studies on shocked achondrites—Shergotty, Zagami, and ALHA77005 (abstract). In *Lunar and Planetary Science XII*, p. 973–975. Lunar and Planetary Institute, Houston.
Sneeringer M. and Hart S. (1978) Sr diffusion in diopside. *EOS (Trans. Amer. Geophys. Union)* **59**, 402.
Steiger R. H. and Jäger E. (1977) Subcommission on geochronology: Convention on the use of decay constants in geo- and cosmochronology. *Earth Planet. Sci. Lett.* **36**, 359–362.
Stöffler D. (1971) Progressive metamorphism and classification of shocked and brecciated crystalline rocks at impact craters. *J. Geophys. Res.* **76**, 5541–5551.
Stöffler D. (1972) Deformation and transformation of rock-forming minerals by natural and experimental shock processes I. Behavior of minerals under shock compression. *Fortschr. Mineral.* **49**, 50–113.
Stolper E. and McSween H. Y. Jr. (1979) Petrology and origin of the Shergottite meteorites. *Geochim. Cosmochim. Acta* **43**, 1475–1598.
Toksöz M. N., Hsui A. T., and Johnston D. H. (1978) Thermal evolution of the terrestrial planets. *Moon and Planets* **18**, 281–320.
Turner G., Cadogan P. H., Jonge C. J. (1973) Argon selenochronology. *Proc. Lunar Sci. Conf. 4th*, p. 1889–1914.
Unruh D. M., Nakamura N., and Tatsumoto M. (1977) History of the Pasamonte achondrite: Relative susceptibility of the Sm–Nd, Rb–Sr, and U–Pb systems to metamorphic events. *Earth Planet. Sci. Lett.* **37**, 1–12.
Weill D. F. and McKay G. A. (1975) The partitioning of Mg, Fe, Sr, Ce, Sm, Eu, and Yb in lunar igneous systems and a possible origin of KREEP by equilibrium partial melting. *Proc. Lunar Sci. Conf. 6th*, p. 1143–1158.

Winzer S. R., Nova D. F., Lum R. K. L., Schuhmann S., Schuhmann P., and Philpotts J. A. (1975) Origin of 78235, a lunar norite cumulate. *Proc. Lunar Sci. Conf. 6th*, p. 1219–1229.
Wolfe S. H. (1971) Potassium-argon ages of the Manicouagan-Mushalagan Lakes structure. *J. Geophys. Res.* **76**, 5424–5436.
York D. (1966) Least-squares fitting of a straight line. *J. Geophys. Res. Canada* **44**, 1079–1086.